The detectors: examples of detector designs

Overall detector designs

- Collider experiment
- Fixed target experiment
- Neutrino experiment
- Cosmic ray experiment

- What determines the size of the detector or:

Why in order to study the smallest systems do we need the largest detectors ?

In the following five examples:

ATLAS+CMS: LHC pp energy frontier experiment

AMS: cosmic ray experiment on a space station

MEG: a fixed target experiment searching for new physics

SNO: an experiment for solar neutrinos.

ATLAS and CMS: the LHC giants!

- Proton-proton collisions at the energy frontier $\sqrt{s} = 14$ TeV with huge luminosity ($L = 10^{34}$ cm^{-2}s^{-1} ➔ $\mu = 25$ evts / bunch crossing): $\boldsymbol{\mu} = L\, \sigma_{tot} / f n_b = 10^{34} \times 100\ \text{mb} \times 25\ 10^{-9}$ s
- General purpose detector not devoted to a single measurement: detect all what you imagine can come out (with momenta from hundreds of MeV up to few TeV):
  - Leptons (electrons, muons)
  - Tau leptons (through their decays, either leptonic or hadronic)
  - Photons
  - Neutrinos (not directly but using the method of the "Missing Energy")
  - Quark/Gluons (not directly but through the so called "Jets")
- Need of data reduction at trigger level: most events are not interesting and you have to choose in a very short time: DAQ rate limited to O(1 kHz)
- Need to discriminate between simultaneous events (pile-up)

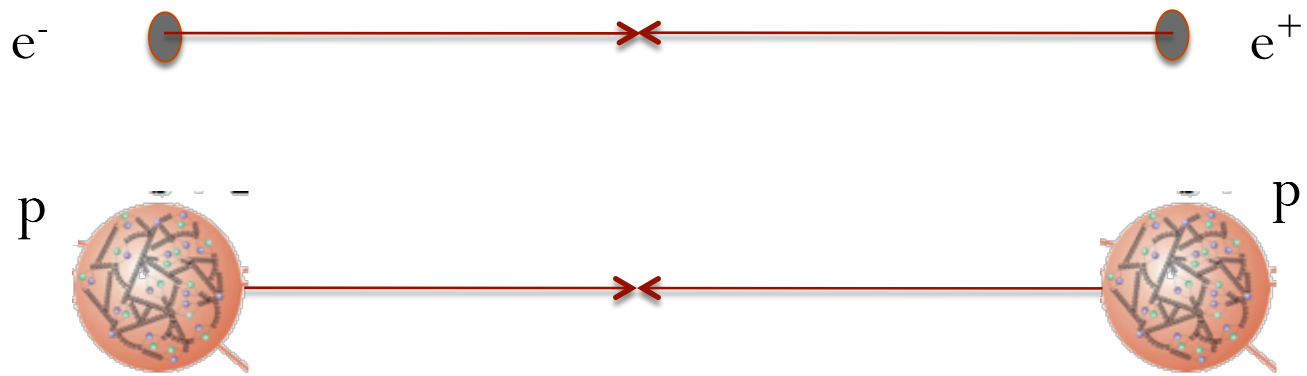

The proton is a complex object done by "partons":

valence quarks / *sea quarks* / *gluons*

s = (center of mass energy of interaction)^2

$\hat{s}$ = (center of mass energy of *elementary* interaction)^2

e^+e^-: interactions btw point-like particles with $\sqrt{\hat{s}} \approx \sqrt{s}$

pp: interactions btw point-like partons with $\sqrt{\hat{s}} << \sqrt{s}$

Parton-parton collision: a+b → d+c.

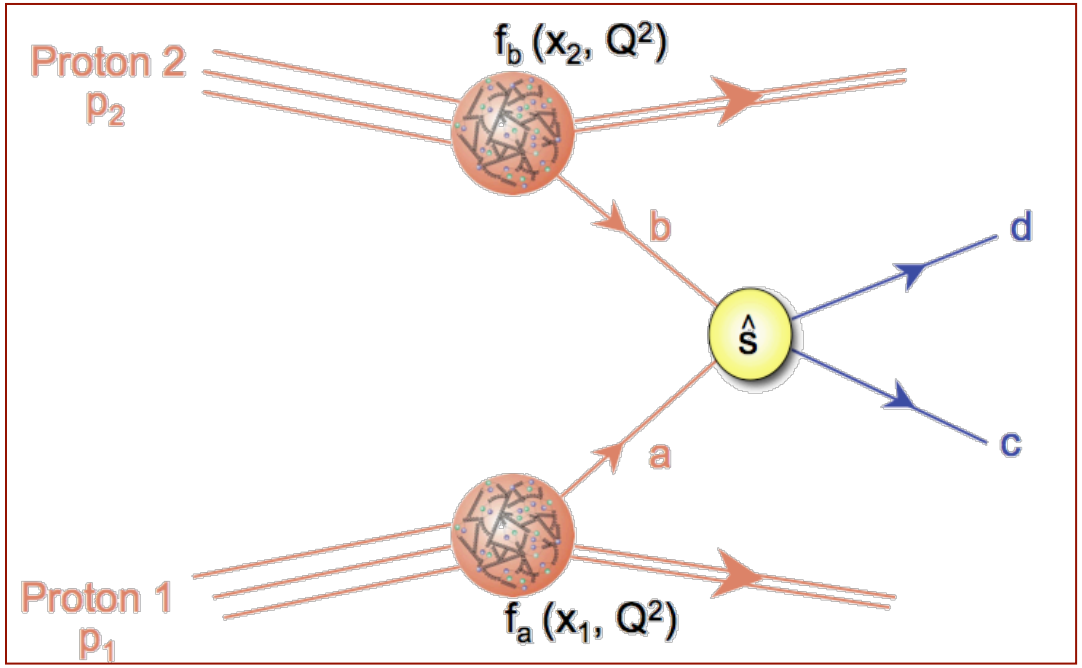

a,b = quarks or gluons;
d,c = quarks, gluons, or leptons, vector bosons,…;
x = fraction of proton momentum carried by each parton;
$\hat{s}$ = parton-parton c.o.m. energy = x_1x_2s (see later);

Theoretical method: the ***factorization theorem***

$$d\sigma(pp \to cd) = \int_0^1 dx_1 dx_2 \sum_{a,b} f_a(x_1,Q^2) f_b(x_2,Q^2) d\hat{\sigma}(ab \to cd)$$

Two ingredients to predict pp cross-sections:

→ proton pdfs (f_a and f_b)

→ $\hat{\sigma}$ “fundamental process” cross-section

parton-parton collisions – let's define the relevant variables

- Parton momentum fractions: x_1 and x_2
  - Assume no transverse momentum
  - Assume mass negligible

$$p_1 = x_1 P = x_1 \frac{\sqrt{s}}{2}(1,0,0,1)$$

$$p_2 = x_2 P = x_2 \frac{\sqrt{s}}{2}(1,0,0,-1)$$

$$\hat{s} = (p_1 + p_2)^2 = x_1 x_2 s$$

- Rapidity: I evaluate the "velocity" of the parton system in the Lab frame:
  - It measures how fast the parton c.o.m. frame moves along z

$$\beta = \frac{p_z}{E} = \frac{(p_1 + p_2)_z}{(p_1 + p_2)_E} = \frac{x_1 - x_2}{x_1 + x_2}$$

$$y = \frac{1}{2}\ln\frac{E + p_z}{E - p_z} = \frac{1}{2}\ln\frac{1+\beta}{1-\beta} = \frac{1}{2}\ln\frac{x_1}{x_2}$$

- Relation between parton rapidity and each single x:

$$x_1 = \sqrt{\frac{\hat{s}}{s}}e^{y}$$

$$x_2 = \sqrt{\frac{\hat{s}}{s}}e^{-y}$$

Rapidity limit for a resonance of mass M

- Suppose that we want to produce in a partonic interaction a resonance of mass M then decaying to a given final state (e.g. pp→Z+X with Z→μμ. Limits in x and y of the collision ?
  - Completely symmetric case: $x_1=x_2=x$

$$x^2 = \frac{M^2}{s}; x = \sqrt{\frac{M^2}{s}}; e^y = 1; y = 0$$

  - Maximally asymmetric case: $x_1=1$, $x_2=x_{min}$

$$x_1 = 1; x_2 = x_{\min} = \frac{M^2}{s}; y_{\max} = \frac{1}{2}\ln\frac{s}{M^2}$$

- Z production at LHC, Tevatron and SpS

	LHC (14 TeV)	Tevatron (1.96 TeV)	SpS (560 GeV)
x_{min}	4.2×10^{-5}	2.1×10^{-3}	0.026
y_{max}	5.03	3.07	1.82

The x-Q^2 plane

→ x – Q^2 plane (Q^2=M=$\hat{s}$) c.o.m. energy of parton interaction. LHC vs. previous experiments showing where PDF are needed to interpret LHC results.

→ NB pp vs. ppbar
ppbar ≈ qqbar collider
pp ≈ gluon collider

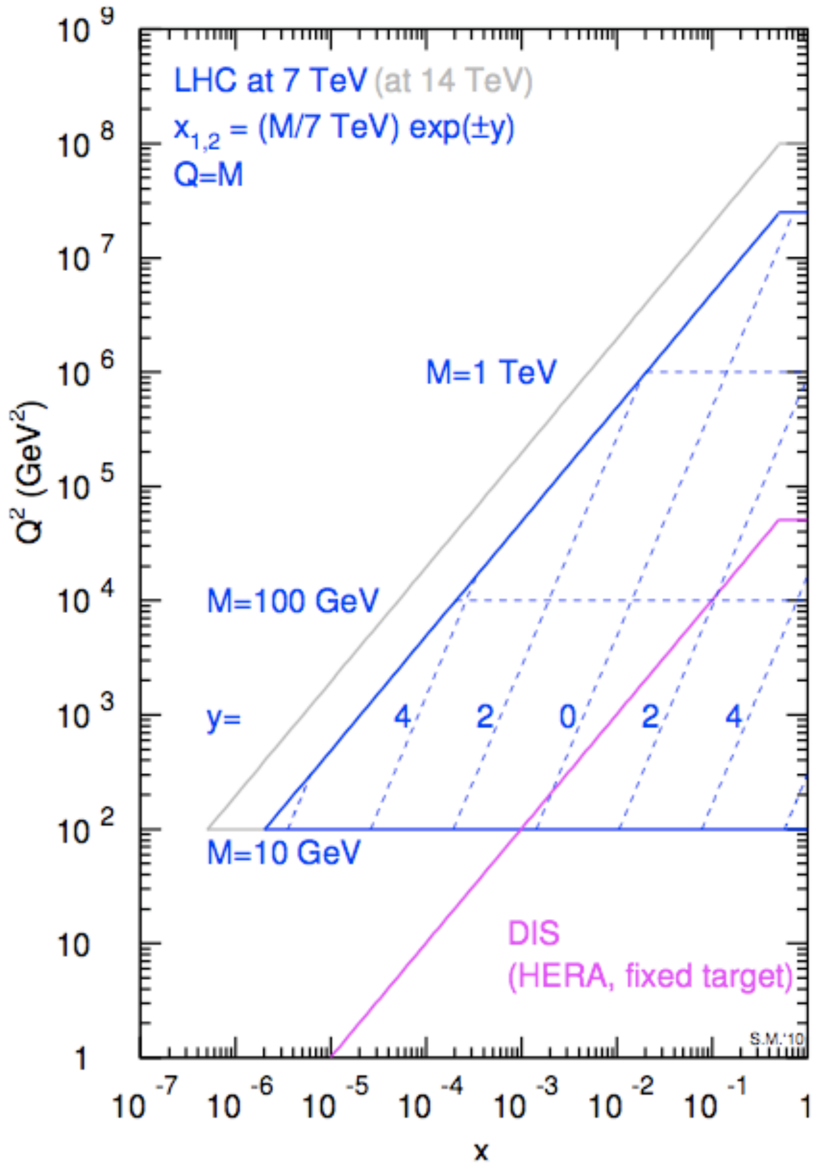

Variables for particles emerging from the collision

- Rapidity y can be defined for any particle emerging from the collision. Let's consider a particle of mass m, energy-momentum E, p and define the rapidity

$$y = \frac{1}{2}\ln\frac{E + p_z}{E - p_z} = \frac{1}{2}\ln\frac{1 + \beta\cos\theta}{1 - \beta\cos\theta}$$

- Pseudorapidity η: it is the rapidity of a particle of 0 mass:

$$\eta = \frac{1}{2}\ln\frac{1 + \beta\cos\theta}{1 - \beta\cos\theta} \rightarrow \frac{1}{2}\ln\frac{1 + \cos\theta}{1 - \cos\theta} = -\ln\tan\frac{\theta}{2}$$

- Transverse energy and momentum:

$$E_T^2 = p_x^2 + p_y^2 + m^2 = E^2 - p_z^2 = \frac{E^2}{\cosh y}; p_T^2 = p_x^2 + p_y^2 = p^2\sin^2\theta$$

- General consideration: Energy and momentum conservation are expected to hold "roughly" in the transverse plane. This gives rise to the concept of missing E_T
- We do not expect momentum conservation on the longitudinal direction.

Properties of the rapidity

- Rapidity y can be defined for any particle emerging from the collision. Let's consider a particle of mass m, energy-momentum E, p and define the rapidity

$$y = \frac{1}{2}\ln\frac{E+p_z}{E-p_z} = \frac{1}{2}\ln\frac{1+\beta\cos\theta}{1-\beta\cos\theta}$$

- Properties
  - If we operate a Lorentz boost along z, y is changed additively (so that Δy the "rapidity gap" is a relativistically invariant quantity):

$$y' = y + y_b$$

$$y_b = \ln\left[\gamma_b\left(1+\beta_b\right)\right]$$

  - If expressed in terms of (p_T, y, ϕ, m) rather than (p_x,p_y,p_z,E) the invariant phase-space volume gets a simpler form:

$$d\tau = \frac{1}{2}dp_T^2 dy d\phi$$

  - so that in case of matrix element uniform over the phase-space, you expect a uniform particle distribution in y and $p_T^{\,2}$.

Invariant mass and missing energy

- The invariant mass of 2 particles emerging from the IP can be written in terms of the above defined variables

$$M_W^2 = 2E_{T1}E_{T2}(\cosh\delta\eta - \cos\delta\phi).$$

- Non-interacting particles such as neutrinos can be detected via a momentum imbalance in the event. But since most of the longitudinal momentum is "lost", the balance is reliable only in the transverse direction. ➔ Missing Transverse Energy $\vec{\not{E}}_T$

$$\vec{\not{E}}_T = -\sum_{k=1}^{Ncl} \vec{E}_{Tk} - \sum_{i=1}^{Nm} \vec{p}_{Ti}$$

$$\vec{E}_{Tk} = \frac{E_k \cos\varphi_k}{\sinh\eta_k}\hat{x} + \frac{E_k \sin\varphi_k}{\sinh\eta_k}\hat{y}$$

Example: W mass constraint: evaluation of neutrino direction

Lastly, since the mass of the W particle is well known [5], we can constrain the invariant mass of the e, ν pair, and solve for the longitudinal momentum of the neutrino. To do this, we can use Eq. (17):

$$M_W^2 = 2E_{T1}E_{T2}(\cosh\delta\eta - \cos\delta\phi).$$

Rewriting this expression, we get

$$\cosh\delta\eta = \frac{M_W^2}{2E_{T1}E_{T2}} + \cos\delta\phi. \tag{21}$$

Solving for $\delta\eta$ gives

$$\delta\eta = ln\frac{r + \sqrt{r^2 - 1}}{2}, \tag{22}$$

where r is the right-hand side of Eq. (21). Because $\delta\eta$ is the difference in pseudorapidity between the electron and the neutrino, there are two solutions to the problem. That is, there is no way of resolving the ambiguity of whether the neutrino is at a lower or higher rapidity relative to the electron as seen from the fact that the hyperbolic cosine $\cosh\delta\eta$ is even in $\delta\eta$. Both solutions are possible, at least in principle.

http://vsharma.ucsd.edu/lhc/Baden-Jets-Kinematics-Writeup.pdf

A detailed look at a p-p collision. What really happens ?

(A) "Real" proton-proton collision
(*pomeron exchange*): 40% of the times

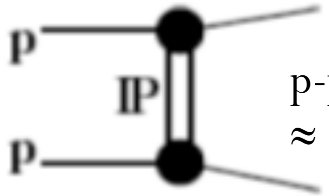

p-p elastic scattering
≈ 25%

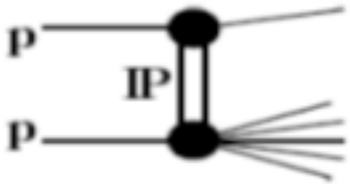

Single diffraction
≈ 10%

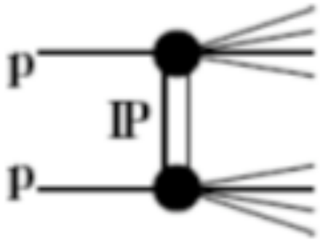

Double diffraction
≈ 1%

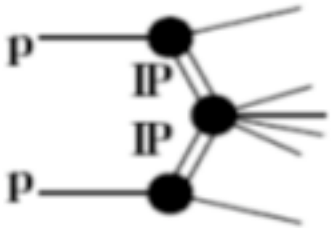

Central diffraction
≈ 1%

(B) Inelastic non-diffractive:
60% of the times

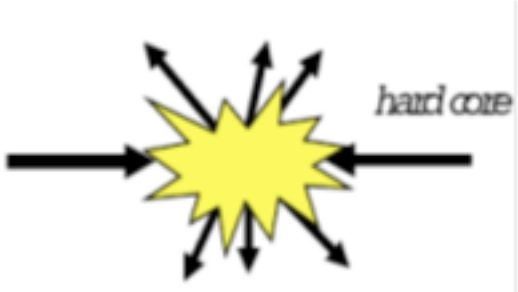

Where is the *fundamental physics* in this picture ?
Among non-diffractive collisions
parton-parton collisions.
Signatures:

proton-proton collision
➔ "forward"

parton-parton collision
➔ "transverse"

Jets - I

Starting from the '70s observation of jet production in e^+e^-, pp and ep collisions. QCD explanation (for e^+e^-):

$e^+e^- \rightarrow$ qqbar $\rightarrow$ hadronisation results in

two jets of hadrons if q (qbar) momenta >> O(100MeV)

NB: in low energy e^+e^- you see multi-hadrons not jets…

2-jet events: qqbar or gg final state that hadronise in 2 jets in back-to-back configuration;

3-jet events: one hard gluon irradiation gives rise to an additional jet (3jet/2jet is a prediction of pQCD)

Several variables can be defined to discriminate "2-jet-like" behaviour wrt isotropic behaviour:

sphericity S 0<S<1

Here, p_{ti} are the transverse momenta of all hadrons in the final state relative to an axis chosen such that the numerator is minimised. (S=0 back-to-back, S=1 isotropic)

$$S = \frac{3\sum_{k=1}^{N} p_{ti}^2}{2\sum_{k=1}^{N} p_i^2}$$

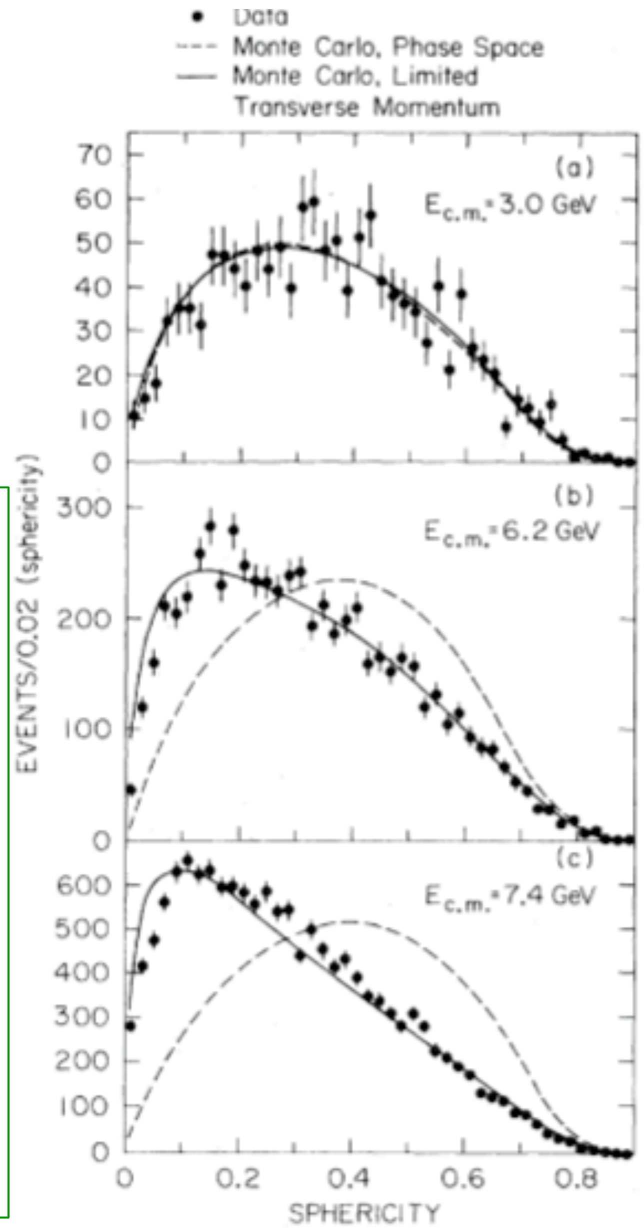

Jets - II

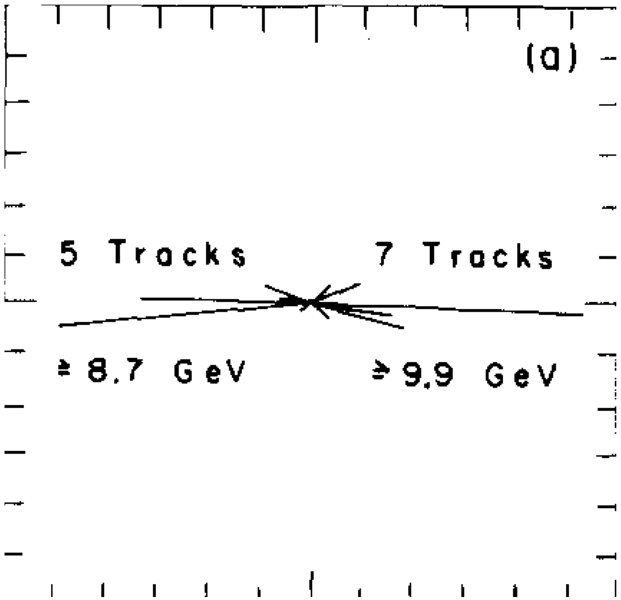
(a)
5 Tracks
7 Tracks
≥ 8.7 GeV
≥ 9.9 GeV

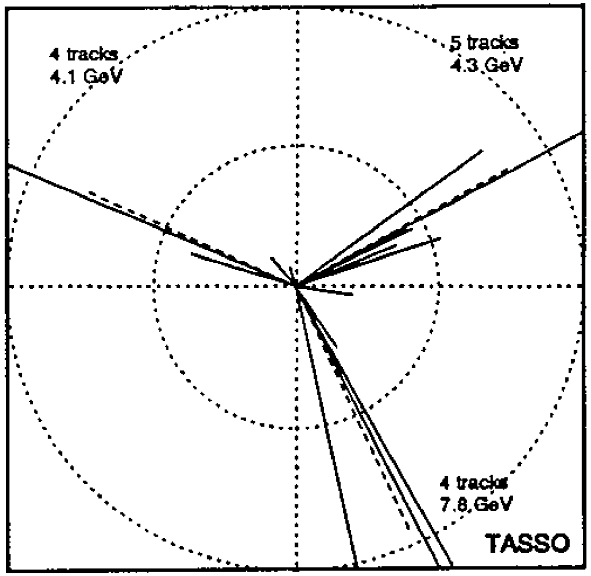
4 tracks
4.1 GeV
5 tracks
4.3 GeV
4 tracks
7.8 GeV
TASSO

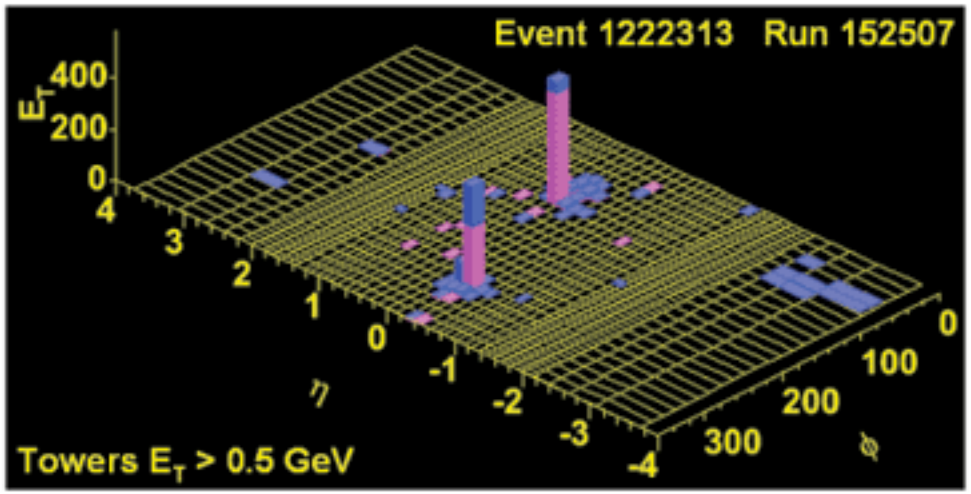
Event 1222313 Run 152507
E_T
400
200
0
4
3
2
1
0
-1
-2
-3
-4
η
0
100
200
300
ϕ
Towers E_T > 0.5 GeV

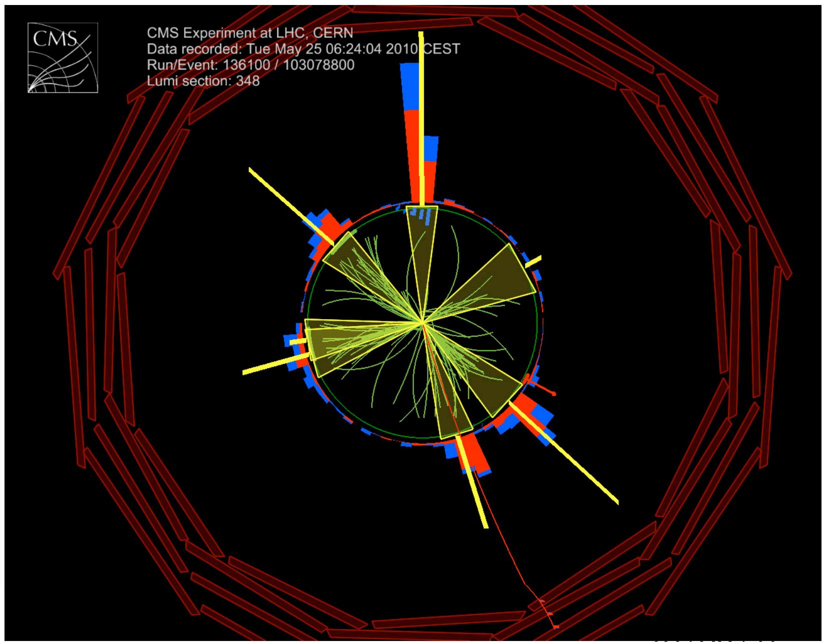
CMS
CMS Experiment at LHC, CERN
Data recorded: Tue May 25 06:24:04 2010 CEST
Run/Event: 136100 / 103078800
Lumi section: 348

Jets - III

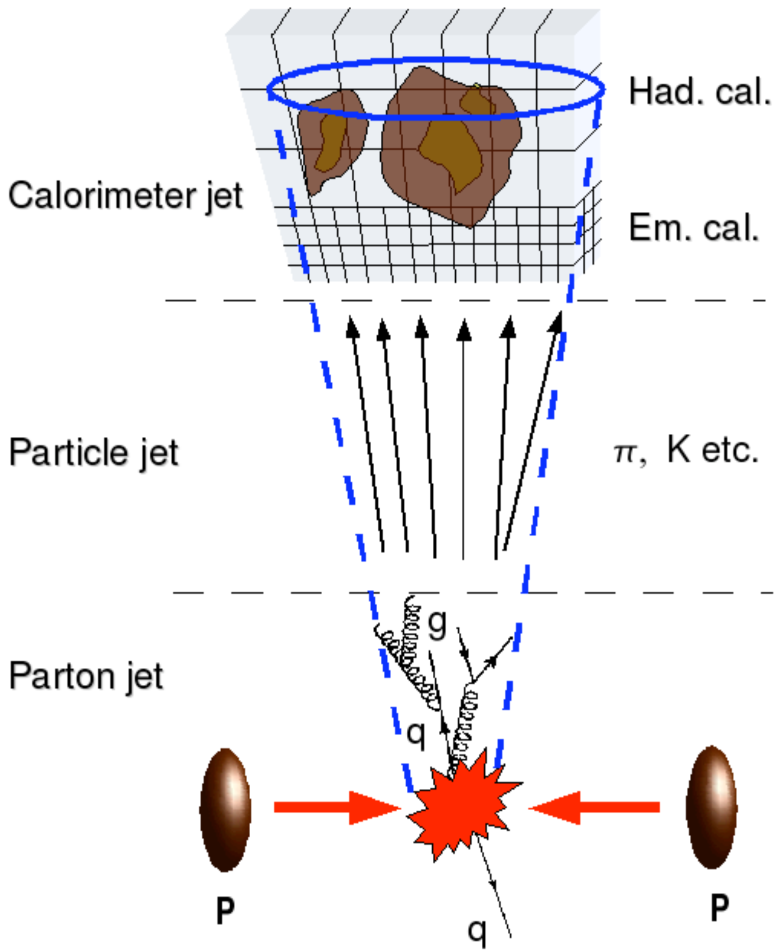

Jet experimental definition:

- based on calorimeter cells
- based on tracks
- → quadri-momentum evaluated (E,p)

Jet algorithms:

- sequential recombination
- cone algorithms
- kT algorithms (against infrared divergences)

$$R = \sqrt{\Delta\eta^2 + \Delta\varphi^2}$$

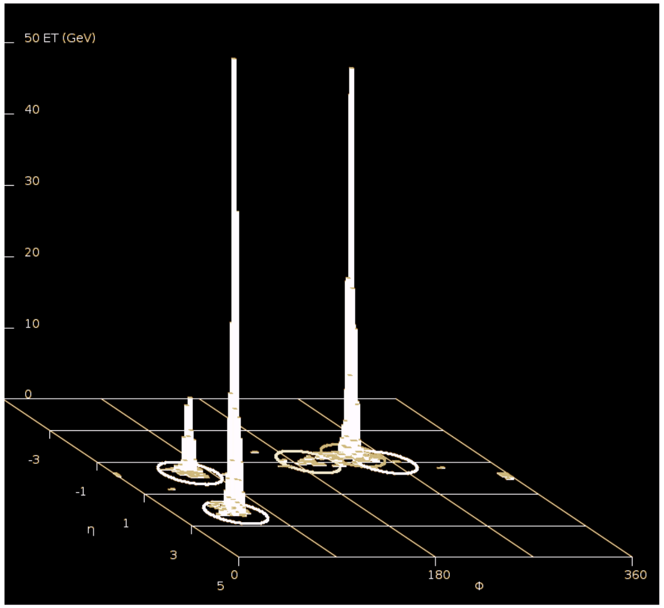

b-Jets

Two main methods to "tag" B-jets:

1) Displaced vertices
2) One or more leptons from semi-leptonic decays. Leptons are not isolated.

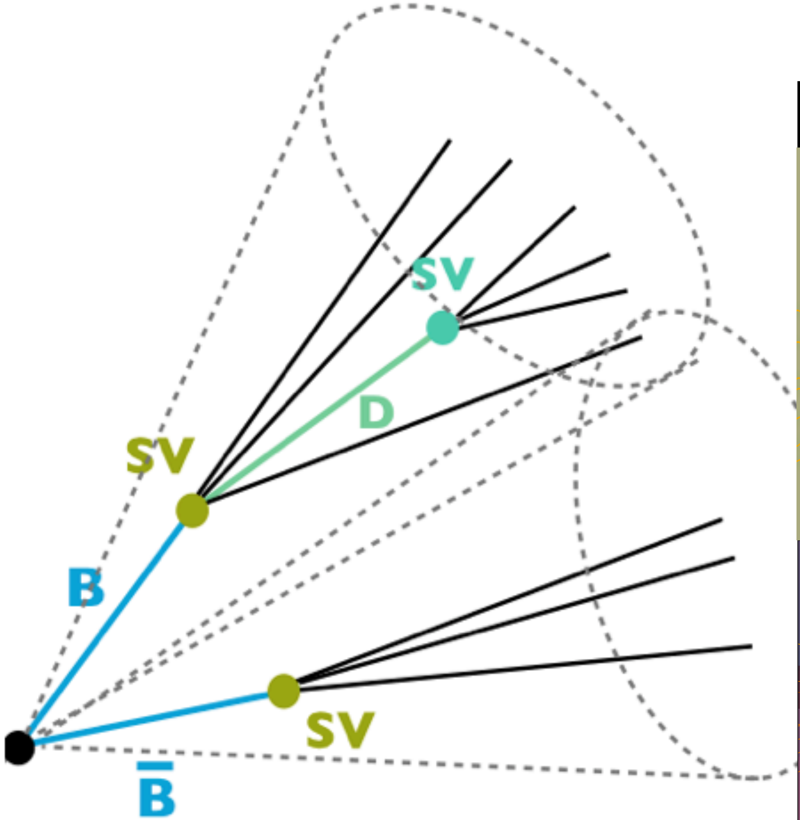

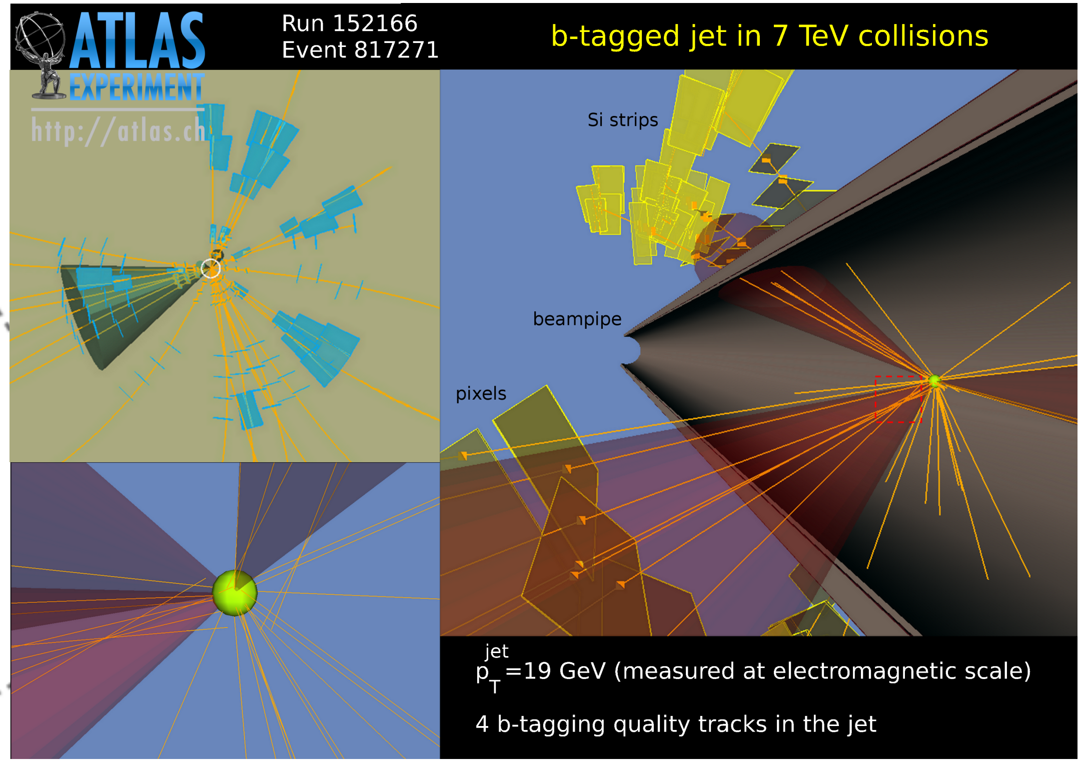

Heavy Ion collisions: the centrality

In heavy ion collisions we define the impact parameter ***b***.

b=0 or small ➔ "central" collision

b large ➔ "peripheral" collision

The "***centrality***" is a measure of ***b***

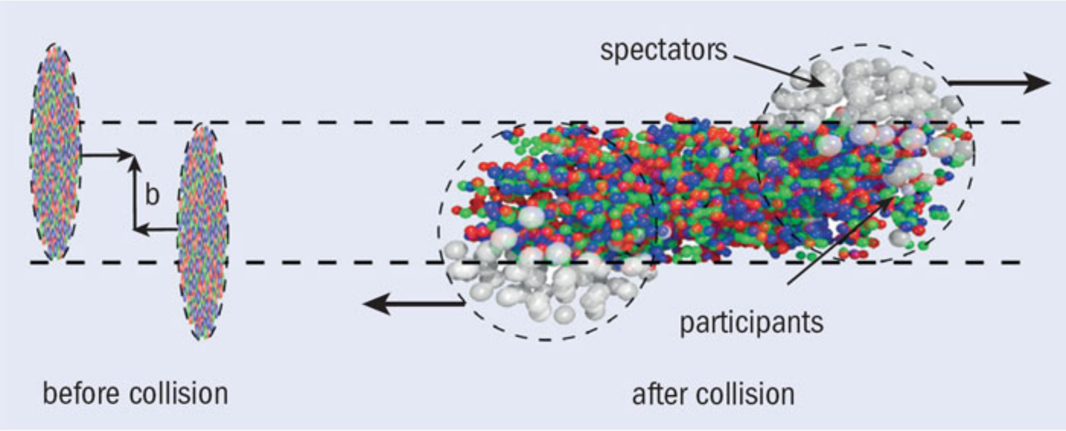

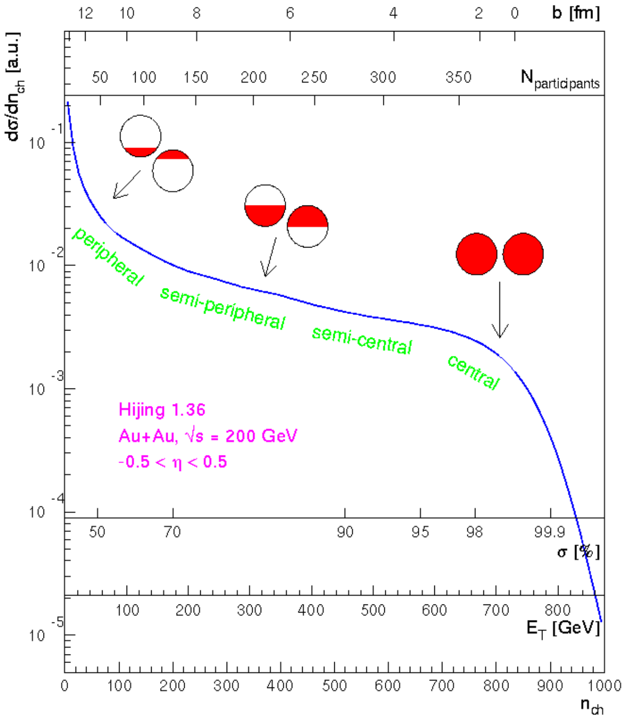

How can we experimentally measure the centrality of each event ?

In a heavy ion collision many particles are produced, mostly in the forward region.

➔ Total energy measured in the Forward detectors

➔ Divide in "percentile" of centralities

Centrality definition

Method: assign to each event a centrality given by the percentile region where the event goes.

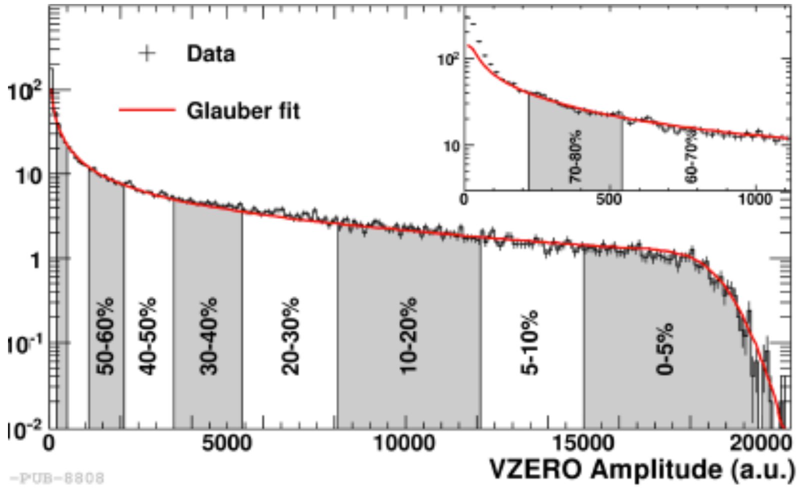

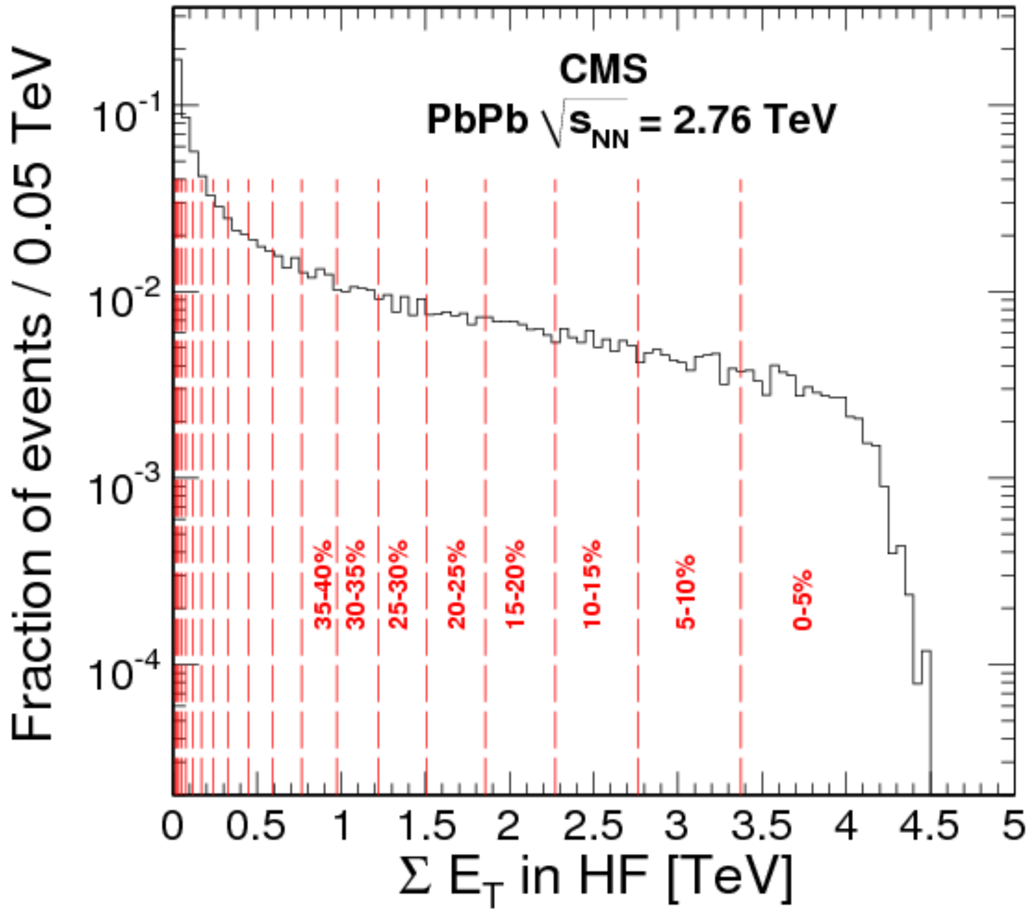

QGP: example of centrality suppression of jets

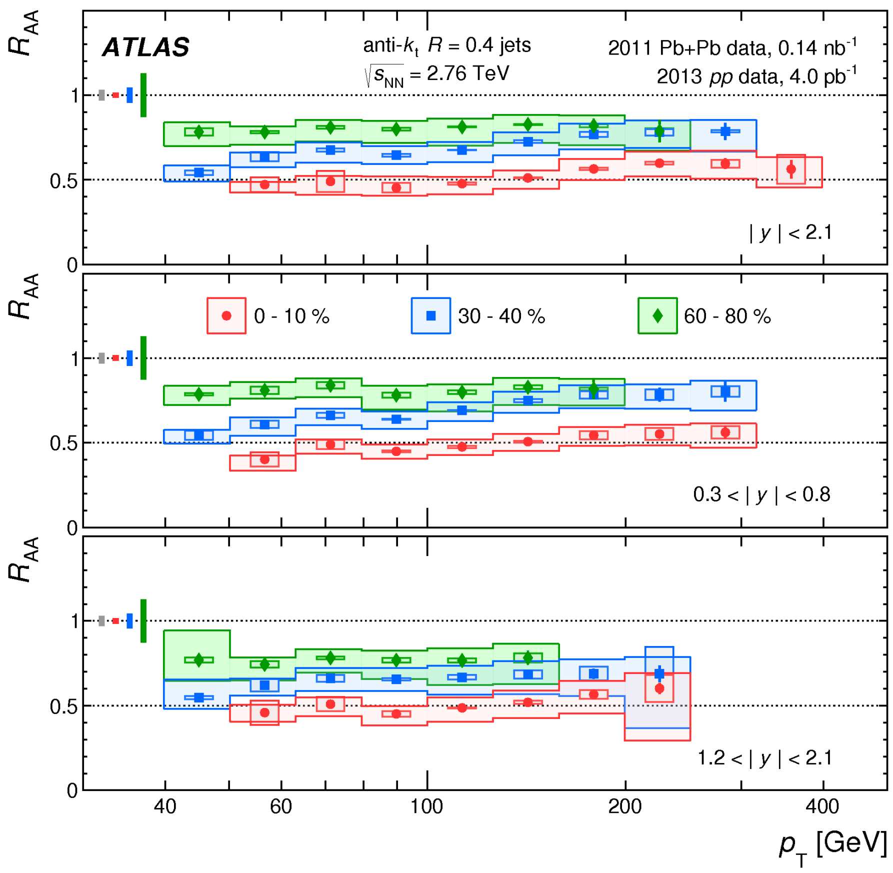

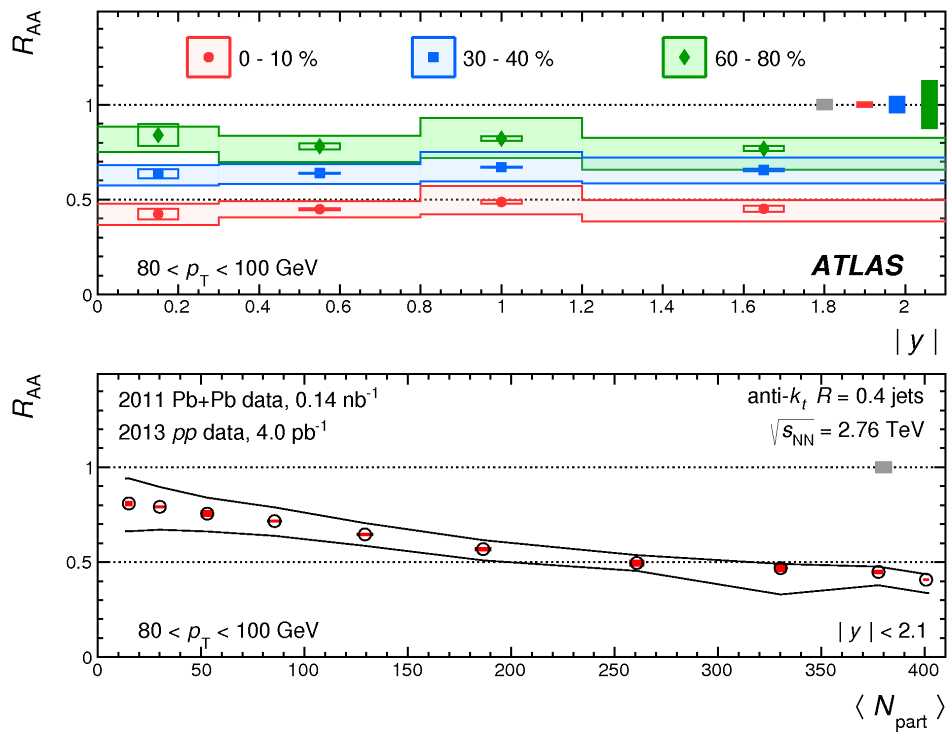

The Giants: ATLAS & CMS

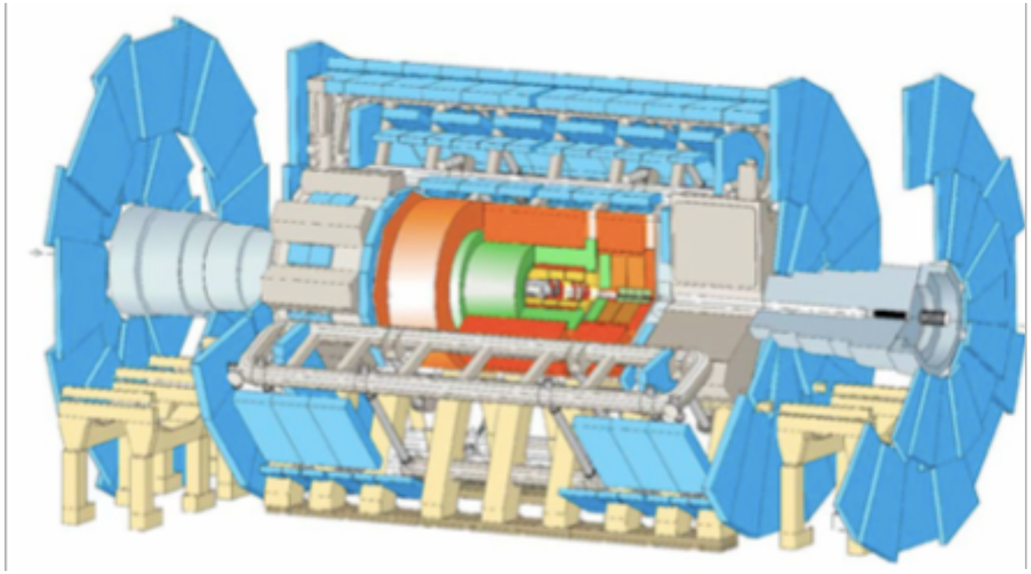

ATLAS (the largest): 46 x 25 m

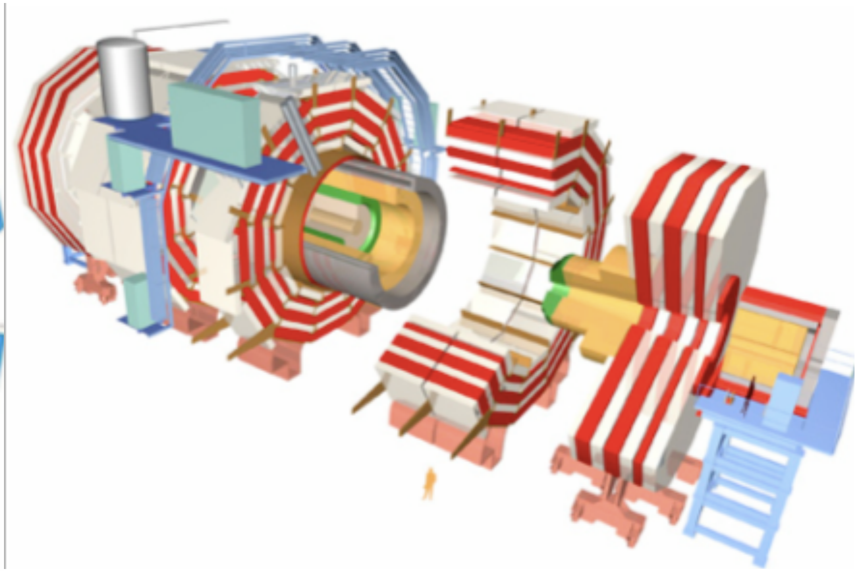

CMS (the heaviest): 12500 tonn

Common structure:	e	μ	Jet	γ	$\not{E}_T$
→ Magnetic Field system	✗	✗			
→ Inner Detector	✗	✗			
→ Electromagnetic Calorimeter	✗		✗	✗	✗
→ Hadronic Calorimeter			✗		✗
→ Muon Spectrometer		✗			

ATLAS

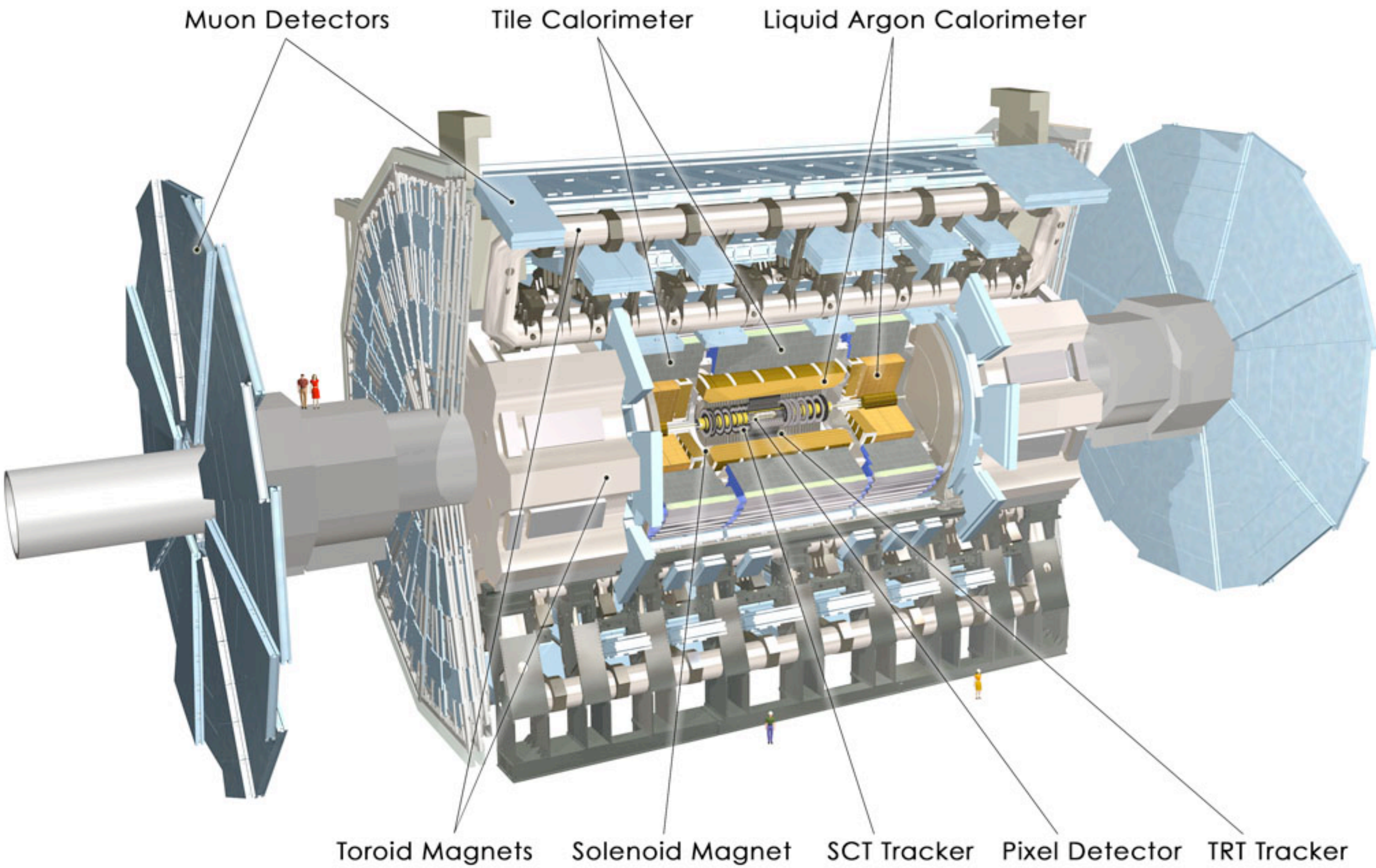
Muon Detectors
Tile Calorimeter
Liquid Argon Calorimeter
Toroid Magnets
Solenoid Magnet
SCT Tracker
Pixel Detector
TRT Tracker

Example: overall structure of the CMS detector

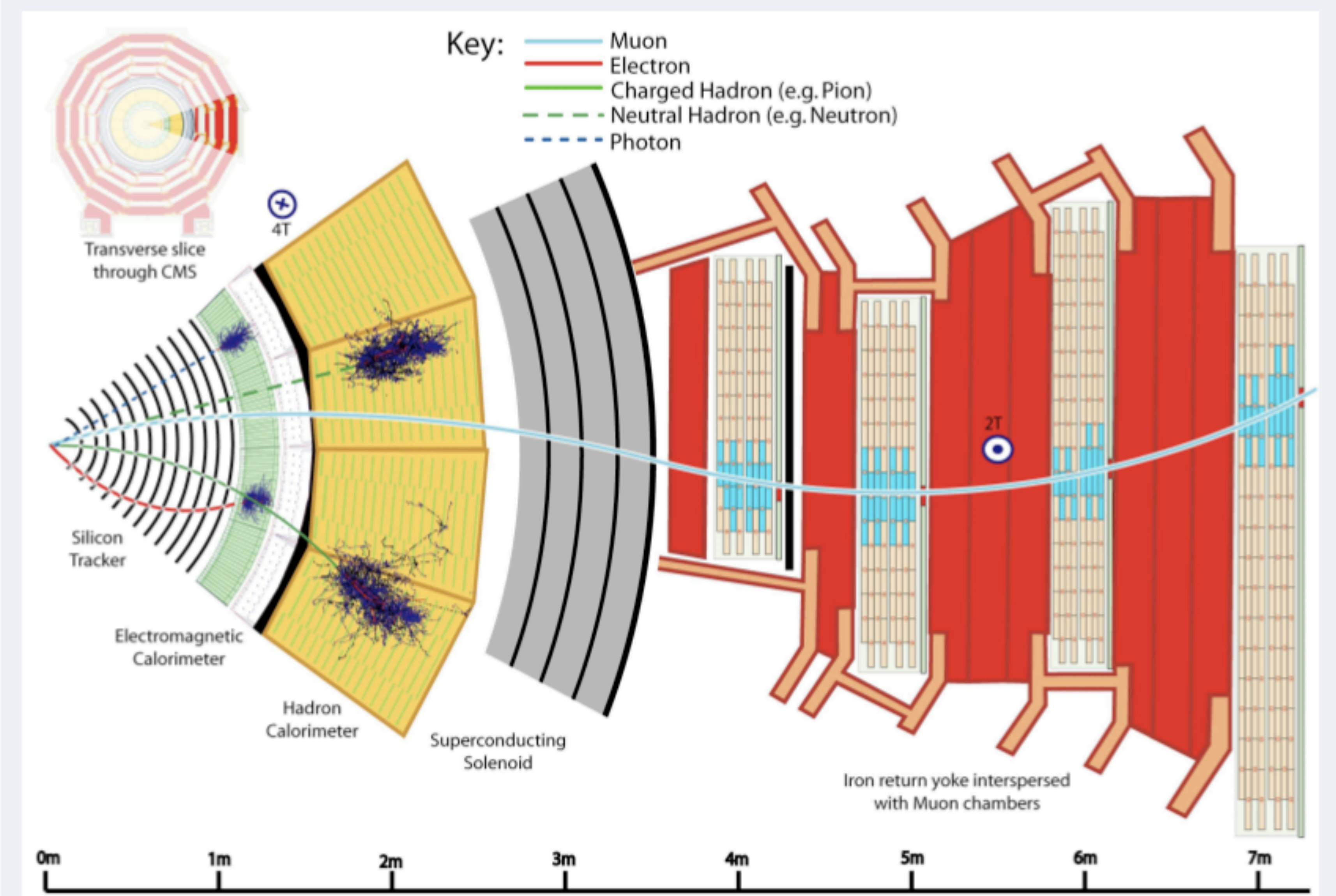

Subdetectors

- Inner Tracker: high space resolution, high resistance to radiation, very high granularity
  - semi-conductor detectors (pixels, silicon strips);
  - gas detectors (ATLAS only) provide electron-hadron separation
- EM calorimetry: good energy resolution, photon identification, high granularity for isolation
- Hadron calorimeter: high eta coverage (for missing mass measurement), moderate granularity to recognize jets
- Muon spectrometer: tagging of muons and standalone trigger. Good momentum resolution (ATLAS only)

ATLAS-CMS: general

TABLE 2 Main design parameters of the ATLAS and CMS detectors

Parameter	**ATLAS**	**CMS**
Total weight (tons)	7000	12,500
Overall diameter (m)	22	15
Overall length (m)	46	20
Magnetic field for tracking (T)	2	4
Solid angle for precision measurements ($\Delta\phi \times \Delta\eta$)	$2\pi \times 5.0$	$2\pi \times 5.0$
Solid angle for energy measurements ($\Delta\phi \times \Delta\eta$)	$2\pi \times 9.6$	$2\pi \times 9.6$
Total cost (million Swiss francs)	550	550

ATLAS-CMS: magnets

TABLE 3 Main parameters of the CMS and ATLAS magnet systems

	CMS	ATLAS		
Parameter	**Solenoid**	**Solenoid**	**Barrel toroid**	**End-cap toroids**
Inner diameter	5.9 m	2.4 m	9.4 m	1.7 m
Outer diameter	6.5 m	2.6 m	20.1 m	10.7 m
Axial length	12.9 m	5.3 m	25.3 m	5.0 m
Number of coils	1	1	8	8
Number of turns per coil	2168	1173	120	116
Conductor size (mm^2)	64×22	30×4.25	57×12	41×12
Bending power	$4\ T \cdot m$	$2\ T \cdot m$	$3\ T \cdot m$	$6\ T \cdot m$
Current	19.5 kA	7.7 kA	20.5 kA	20.0 kA
Stored energy	2700 MJ	38 MJ	1080 MJ	206 MJ

How muons are detected at LHC

→ The calorimeters provide a "natural" muon filter;
→ The magnetic field system. ATLAS and CMS have different approaches

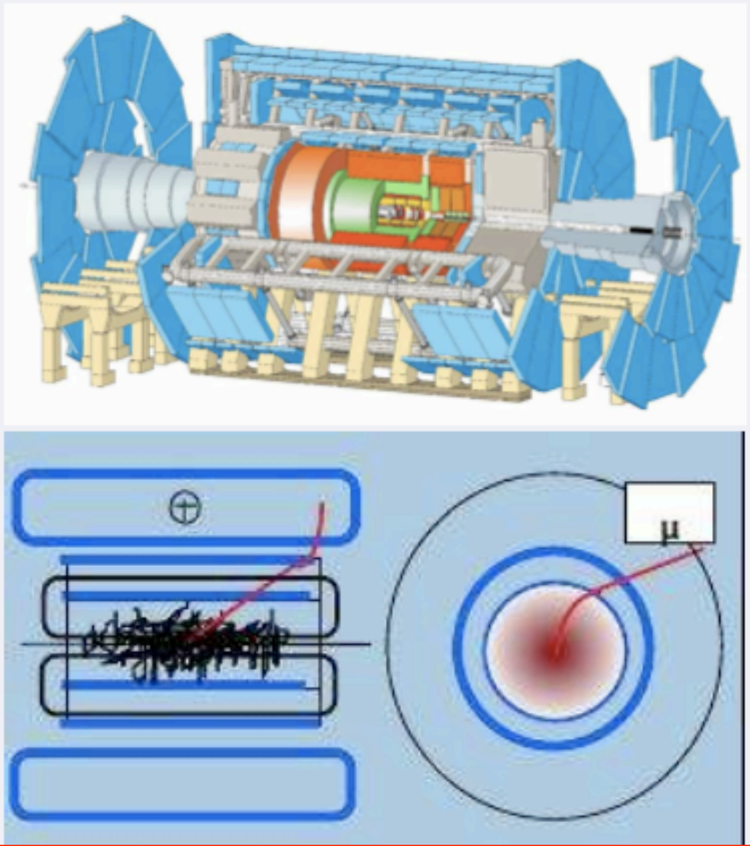

ATLAS: inner solenoid + outer toroids

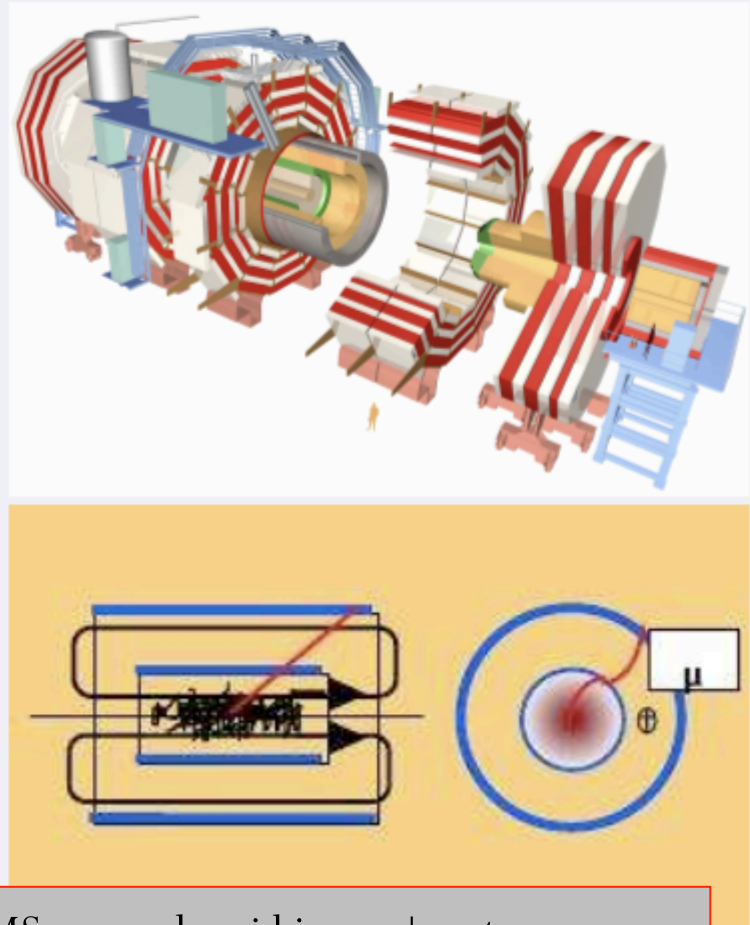

CMS: one solenoid inner + outer (reversed direction)

ATLAS-CMS: inner tracker

TABLE 4 Main parameters of the ATLAS and CMS tracking systems (see Table 6 for details of the pixel systems)

Parameter	ATLAS	CMS
Dimensions (cm)		
-radius of outermost measurement	101–107	107–110
-radius of innermost measurement	5.0	4.4
-total active length	560	540
Magnetic field B (T)	2	4
BR^2 ($T \cdot m^2$)	2.0 to 2.3	4.6 to 4.8
Total power on detector (kW)	70	60
Total weight in tracker volume (kg)	≈4500	≈3700
Total material (X/X_0)		
-at $\eta \approx 0$ (minimum material)	0.3	0.4
-at $\eta \approx 1.7$ (maximum material)	1.2	1.5
-at $\eta \approx 2.5$ (edge of acceptance)	0.5	0.8
Total material (λ/λ_0 at max)	0.35	0.42
Silicon microstrip detectors		
-number of hits per track	8	14
-radius of innermost meas. (cm)	30	20
-total active area of silicon (m^2)	60	200
-wafer thickness (microns)	280	320/500
-total number of channels	6.2×10^6	9.6×10^6
-cell size (μm in $R\phi$ × cm in z/R)	80×12	$80/120 \times 10$
-cell size (μm in $R\phi$ × cm in z/R)		and $120/180 \times 25$
Straw drift tubes (ATLAS only)		
-number of hits per track ($\lvert\eta\rvert < 1.8$)	35	
-total number of channels	350,000	
-cell size (mm in $R\phi$ × cm in z)	4×70 (barrel)	
	4×40 (end caps)	

ATLAS-CMS: pixel

TABLE 6 Main parameters of the ATLAS and CMS pixel systems

	ATLAS	**CMS**
Number of hits per track	3	3
Total number of channels	$80\ 10^6$	$66\ 10^6$
Pixel size (μm in $R\phi$ × μm in z/R)	50×400	100×150
Lorentz angle (degrees), initial to end	12 to 4	26 to 8
Tilt in $R\phi$ (degrees)	20 (only barrel)	20 (only end cap)
Total active area of silicon (m^2)	1.7 (n^+/n)	1.0 (n^+/n)
Sensor thickness (μm)	250	285
Total number of modules	1744 (288 in disks)	1440 (672 in disks)
Barrel layer radii (cm)	5.1, 8.9, 12.3	4.4, 7.3, 10.2
Disk layer min. to max. radii (cm)	8.9 to 15.0	6.0 to 15.0
Disk positions in z (cm)	49.5, 58.0, 65.0	34.5, 46.5
Signal-to-noise ratio for minimum ionizing particles (day 1)	120	130
Total fluence at L = 10^{34} (n_{eq}/cm^2/year) at radius of 4–5 cm (innermost layer)	3×10^{14}	3×10^{14}
Signal-to-noise ratio (after 10^{15} n_{eq}/cm^2)	80	80
Resolution in $R\phi$ (μm)	≈10	≈10
Resolution in z/R (μm)	≈100	≈20

ATLAS-CMS: ECAL

TABLE 8 Main parameters of the ATLAS and CMS electromagnetic calorimeters

	ATLAS		CMS	
Technology	Lead/LAr accordion		$PbWO_4$ scintillating crystals	
Channels	Barrel	End caps	Barrel	End caps
	110,208	63,744	61,200	14,648
Granularity	$\Delta\eta \times \Delta\phi$		$\Delta\eta \times \Delta\phi$	
Presampler	0.025×0.1	0.025×0.1		
Strips/ Si-preshower	0.003×0.1	0.003×0.1 to 0.006×0.1		32×32 Si-strips per 4 crystals
Main sampling	0.025×0.025	0.025×0.025	0.017×0.017	0.018×0.003 to 0.088×0.015
Back	0.05×0.025	0.05×0.025		
Depth	Barrel	End caps	Barrel	End caps
Presampler (LAr)	10 mm	2×2 mm		
Strips/ Si-preshower	$\approx 4.3\ X_0$	$\approx 4.0\ X_0$		$3\ X_0$
Main sampling	$\approx 16\ X_0$	$\approx 20\ X_0$	$26\ X_0$	$25\ X_0$
Back	$\approx 2\ X_0$	$\approx 2\ X_0$		
Noise per cluster	250 MeV	250 MeV	200 MeV	600 MeV
Intrinsic resolution	Barrel	End caps	Barrel	End caps
Stochastic term a	10%	10 to 12%	3%	5.5%
Local constant term b	0.2%	0.35%	0.5%	0.5%

Note the presence of the silicon preshower detector in front of the CMS end-cap crystals, which have a variable granularity because of their fixed geometrical size of 29×29 mm^2. The intrinsic energy resolutions are quoted as parametrizations of the type $\sigma(E)/E = a/\sqrt{E} \oplus b$. For the ATLAS EM barrel and end-cap calorimeters and for the CMS barrel crystals, the numbers quoted are based on stand-alone test-beam measurements.

ATLAS-CMS: HCAL

TABLE 9 Main parameters of the ATLAS and CMS hadronic calorimeters

	ATLAS	CMS
Technology		
Barrel/Ext. barrel	14 mm iron/3 mm scint.	50 mm brass/3.7 mm scint.
End caps	25–50 mm copper/8.5 mm LAr	78 mm brass/3.7 mm scint.
Forward	Copper (front) - Tungsten (back)/0.25–0.50 mm LAr	Steel/0.6 mm quartz
Channels		
Barrel/Ext. barrel	9852	2592
End caps	5632	2592
Forward	3524	1728
Granularity ($\Delta\eta \times \Delta\phi$)		
Barrel/Ext. barrel	0.1×0.1 to 0.2×0.1	0.087×0.087
End caps	0.1×0.1 to 0.2×0.2	0.087×0.087 to 0.18×0.175
Forward	0.2×0.2	0.175×0.175
Samplings ($\Delta\eta \times \Delta\phi$)		
Barrel/Ext. barrel	3	1
End caps	4	2
Forward	3	2
Abs. lengths (min.-max.)		
Barrel/Ext. barrel	9.7–13.0	7.2–11.0 10–14 (with coil/HO)
End caps	9.7–12.5	9.0–10.0
Forward	9.5–10.5	9.8

Note that the CMS barrel calorimeter (HB) is complemented by a tail catcher behind the coil (HO) to minimize problems with longitudinal leakage of high-energy particles in jets.

ATLAS-CMS: calorimeters

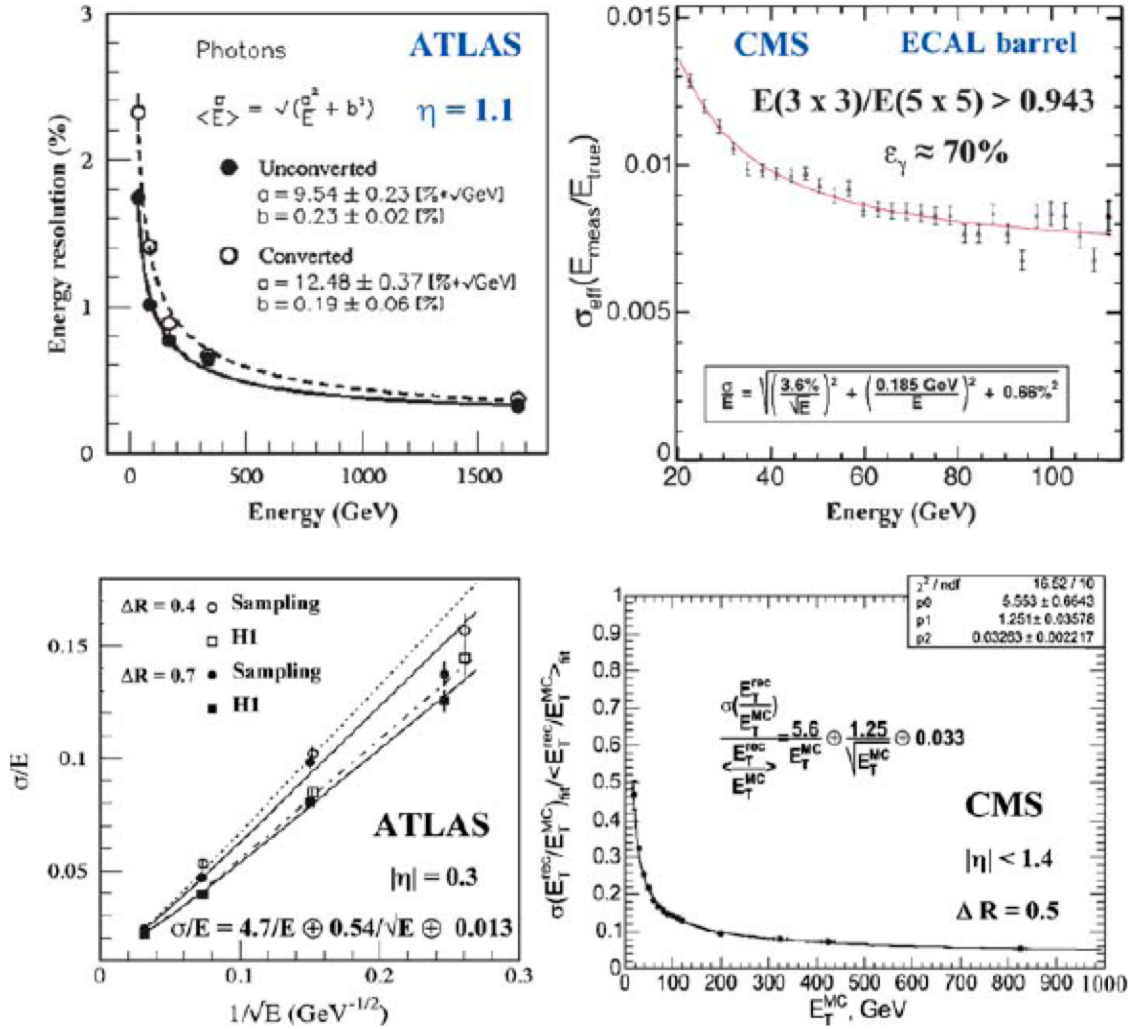

ATLAS-CMS: muons

TABLE 11 Main parameters of the ATLAS and CMS muon chambers

	ATLAS	**CMS**
Drift Tubes	MDTs	DTs
-Coverage	$\|\eta\| < 2.0$	$\eta\| < 1.2$
-Number of chambers	1170	250
-Number of channels	354,000	172,000
-Function	Precision measurement	Precision measurement, triggering
Cathode Strip Chambers		
-Coverage	$2.0 < \|\eta\| < 2.7$	$1.2 < \|\eta\| < 2.4$
-Number of chambers	32	468
-Number of channels	31,000	500,000
-Function	Precision measurement	Precision measurement, triggering
Resistive Plate Chambers		
-Coverage	$\|\eta\| < 1.05$	$\|\eta\| < 2.1$
-Number of chambers	1112	912
-Number of channels	374,000	160,000
-Function	Triggering, second coordinate	Triggering
Thin Gap Chambers		
-Coverage	$1.05 < \|\eta\| < 2.4$	—
-Number of chambers	1578	—
-Number of channels	322,000	—
-Function	Triggering, second coordinate	—

ATLAS-CMS: muon momentum resolutions

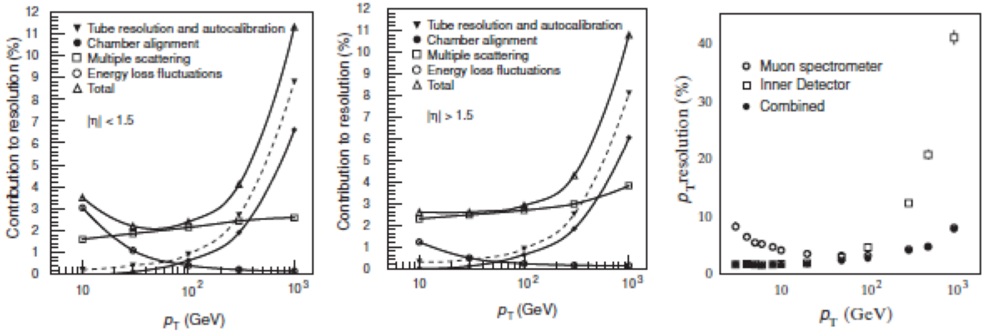

Figure 24 Expected performance of the ATLAS muon measurement. Contributions to the momentum resolution in the muon spectrometer averaged over $|\eta| < 1.5$ (*left*) and $1.5 < |\eta| < 2.7$ (*center*). (*Right*) Muon momentum resolution expected from muon spectrometer, Inner Detector, and their combination together as a function of muon transverse mor

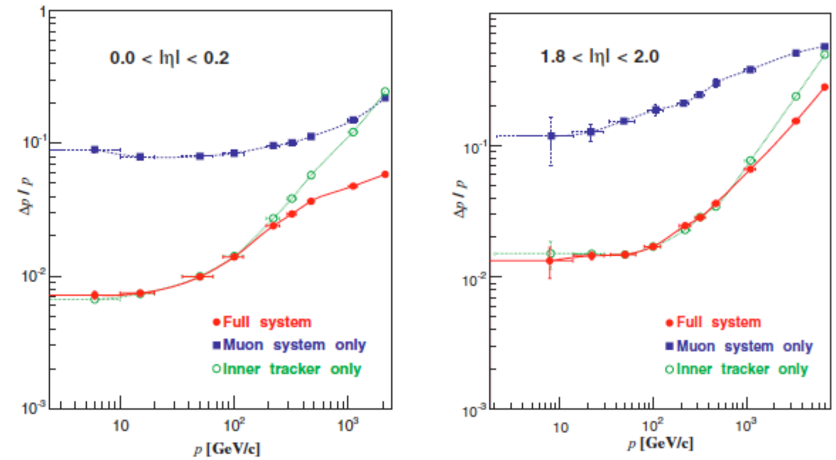

Figure 25 Expected performance of the CMS muon measurement. The muon momentum resolution is plotted versus momentum using the muon system only, the inner tracker only, or their combination (full system). (*Left*) Barrel, with $|\eta| < 0.2$. (*Right*) End cap, with $1.8 < |\eta| < 2.0$.

ATLAS vs. CMS

- Driven by the goal to achieve a high-precision stand-alone momentum measurement of muons "achieved using an arrangement of a small-radius thin-walled solenoid integrated into the cryostat of the barrel ECAL, surrounded by a system of three large air-core toroids, situated outside the ATLAS calorimeter systems, and generating the magnetic field for the muon spectrometer."
- Electrons
  - ECAL, and matching between the E,p measured by ECAL and tracker
  - Also enhenced by ATLAS TRT's ability to separate electrons from charged pions
- ATLAS solenoid is located just in front of the barrel ECAL, resulting in significant energy loss by electrons and photons in the material in front of the active ECAL
- HCAL is thick enough: good jet and missing E_T measurement

- A single magnet with "a high magnetic field in the tracker volume for all precision momentum measurements, and a high enough return flux in the iron outside the magnet to provide a muon trigger and a second muon momentum measurement."
- Invested in highest possible magnetic filed: 4T → better tracking resolution than ATLAS
  - Inner tracker consisting of all silicon detectors
- γ/Electrons → High resolution crystals, better than ATLAS
- The full EM calorimetry and most of its hadronic alorimetry are situated inside the solenoid coil and therefore bathed in the strong 4T magnetic field
- HCAL. The strong constraints imposed by the CMS solenoid have resulted in a barrel hadronic calorimeter with insufficient absorption (~ 7 absorption lengths). So a tail catcher (HO) has been added around the coil to complement the HB. But still, over-all, CMS jet resolution is worse than ATLAS.

An important quest for pp experiments: the ***Trigger***

$$\dot{N} = \sigma_{tot} L \approx 10^{-25} cm^2 \times 10^{32 \div 34} cm^{-2} s^{-1} = 10\,MHz \div 1GHz$$

bunch crossing rate = 40 MHz
➔ every b.c. contains at least
an interaction (25/b.c. at max L)

- Technically impossible and physically not interesting to register all b.c.s
- Retain only "interesting" b.c.

  ➔ TRIGGER = online decision:
  take or reject the b.c.
- *Decision has to be fast;*
- *Criteria have to be flexible and scalable;*
- *Thresholds have to be defined.*

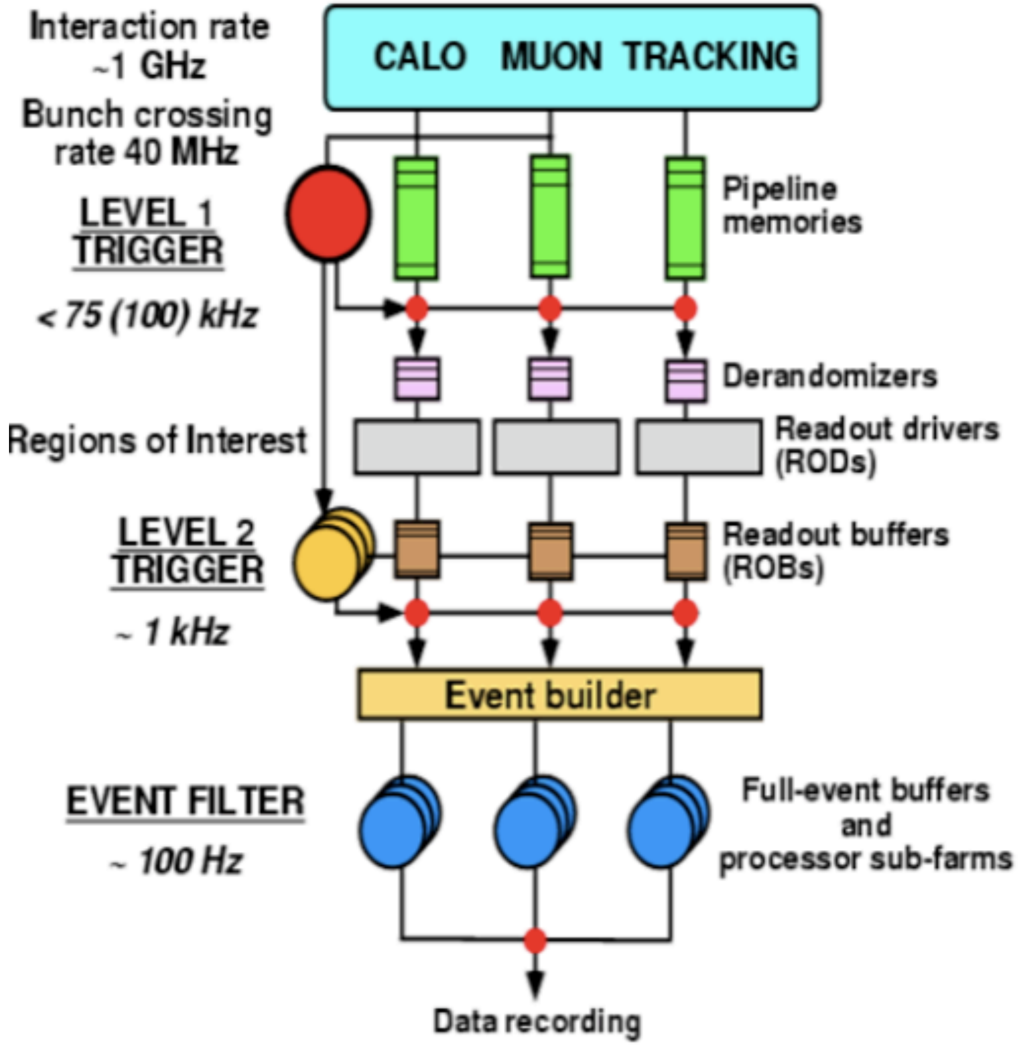

AMS

- Aim of the experiment:
  - measure e^+/e^- spectra, fluxes and ratios;
  - measure proton and ions spectra fluxes and ratios
  - look for possible dark matter signals
  - measure flux of primary anti-protons
- Detector requirements
  - measure the sign of the charge (e^+/e^- discrimination)
  - measure the Z of a ion
  - measure particle velocity

AMS: an experiment on the space station.

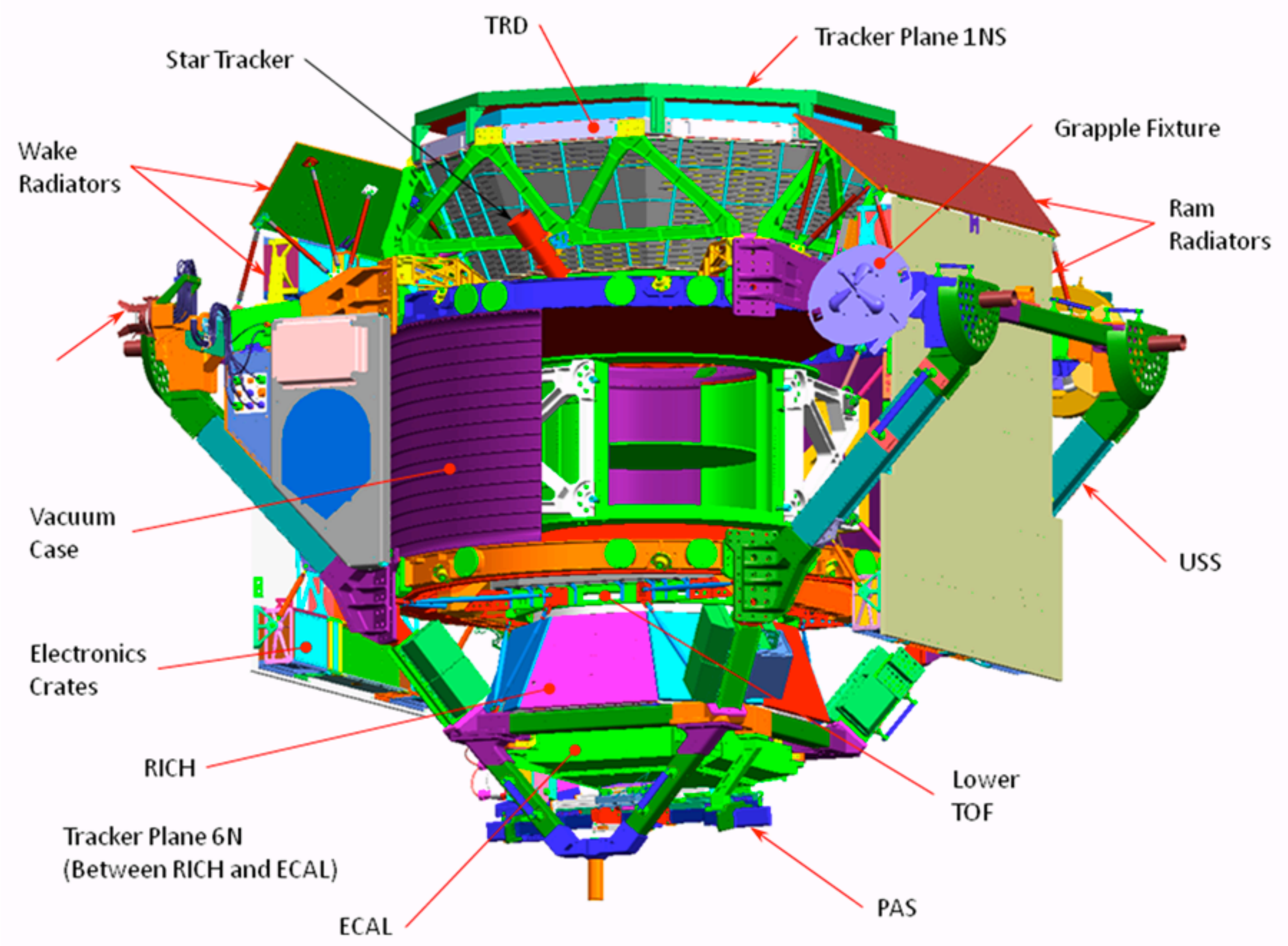

AMS – subdetectors.

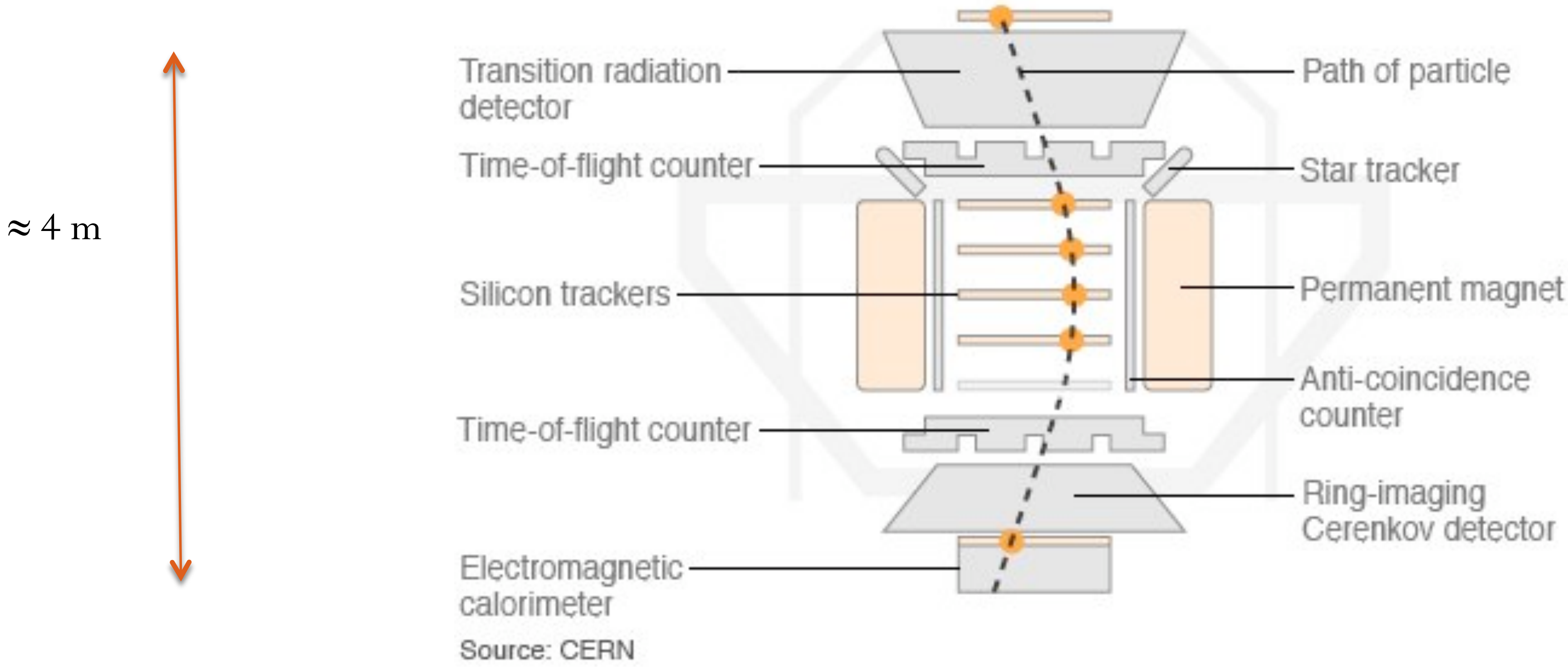

AMS-02
18 years on the ISS
TRD
Identify e+, e-
TOF
Z, E
Magnet
±Z
Silicon Tracker
Z, P
RICH
Z, E
ECAL
E of e+, e-, γ
1
TRD
TOF
2
3-4
5-6
7-8
Tracker
TOF
RICH
9
ECAL

AMS - Events

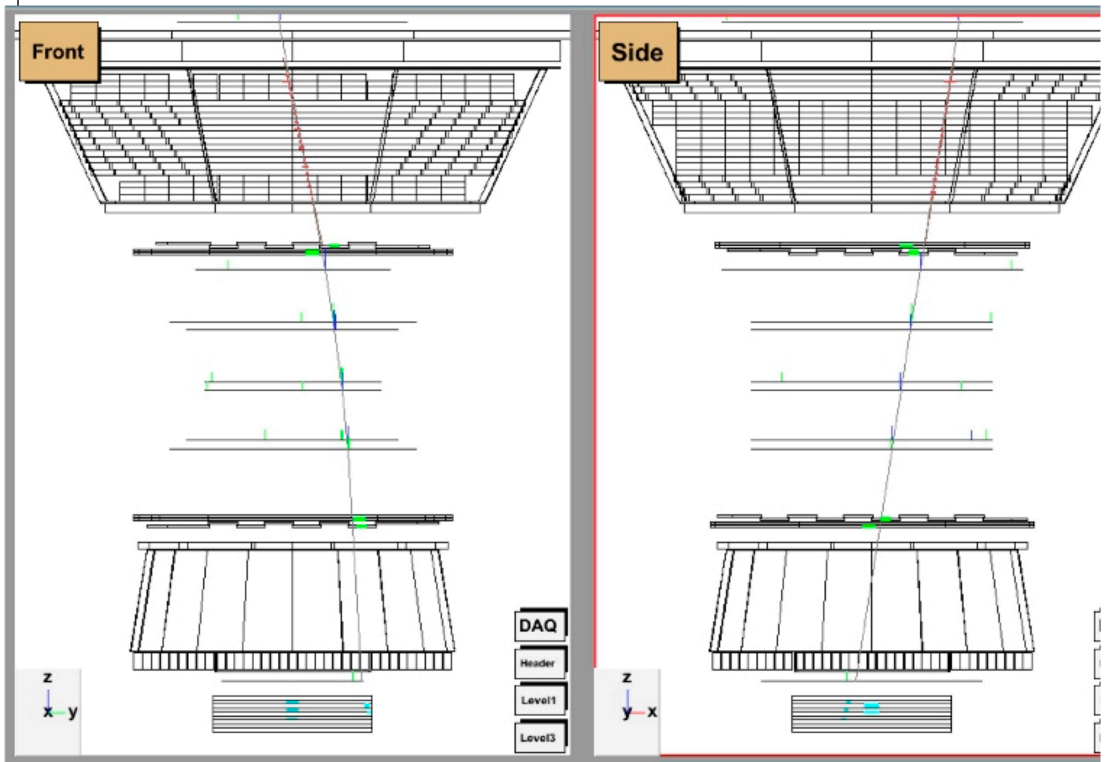

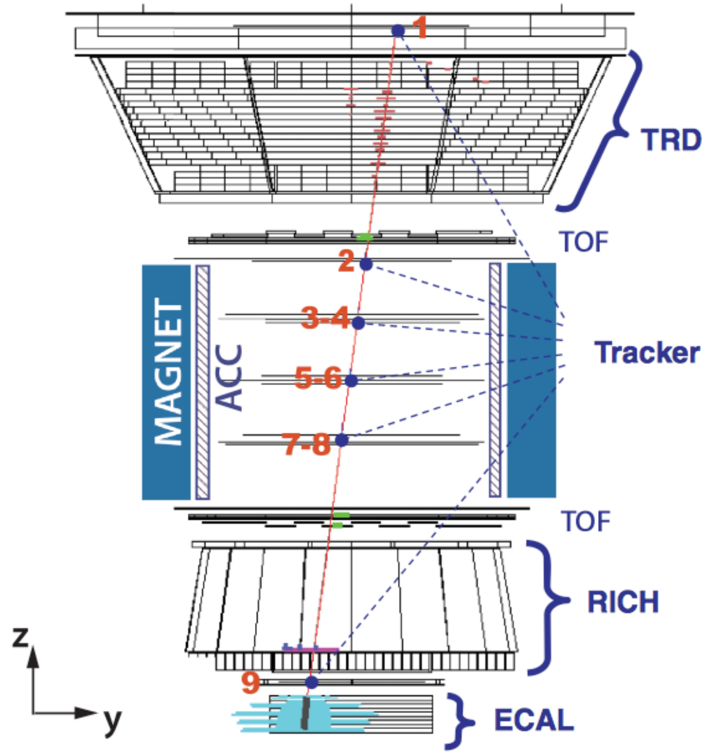

FIG. 1 (color). A 1.03 TeV electron event as measured by the AMS detector on the ISS in the bending (y-z) plane. Tracker planes 1–9 measure the particle charge and momentum. The TRD identifies the particle as an electron. The TOF measures the charge and ensures that the particle is downward-going. The RICH independently measures the charge and velocity. The ECAL measures the 3D shower profile, independently identifies the particle as an electron, and measures its energy. An electron is identified by (i) an electron signal in the TRD, (ii) an electron signal in the ECAL, and (iii) the matching of the ECAL shower energy and the momentum measured with the tracker and magnet.

AMS – subdetector functionalities

AMS: A TeV Magnetic Spectrometer in Space

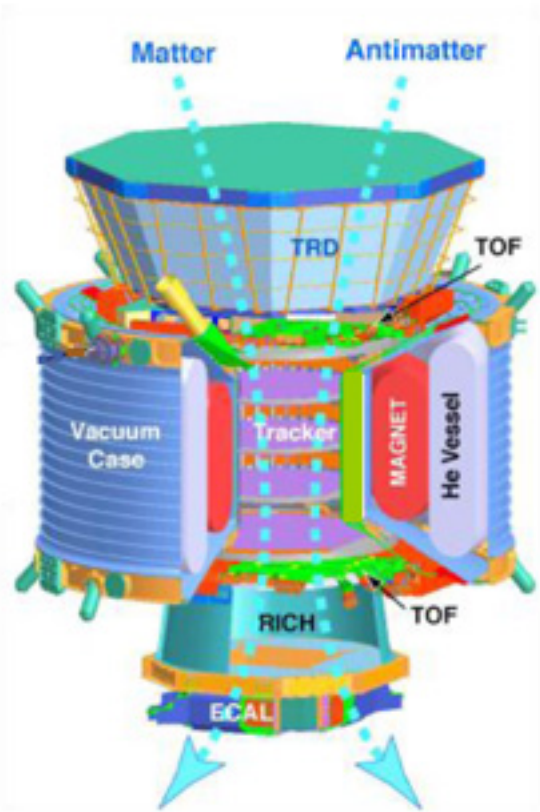

Data Signature of Various Particles in Each Detector

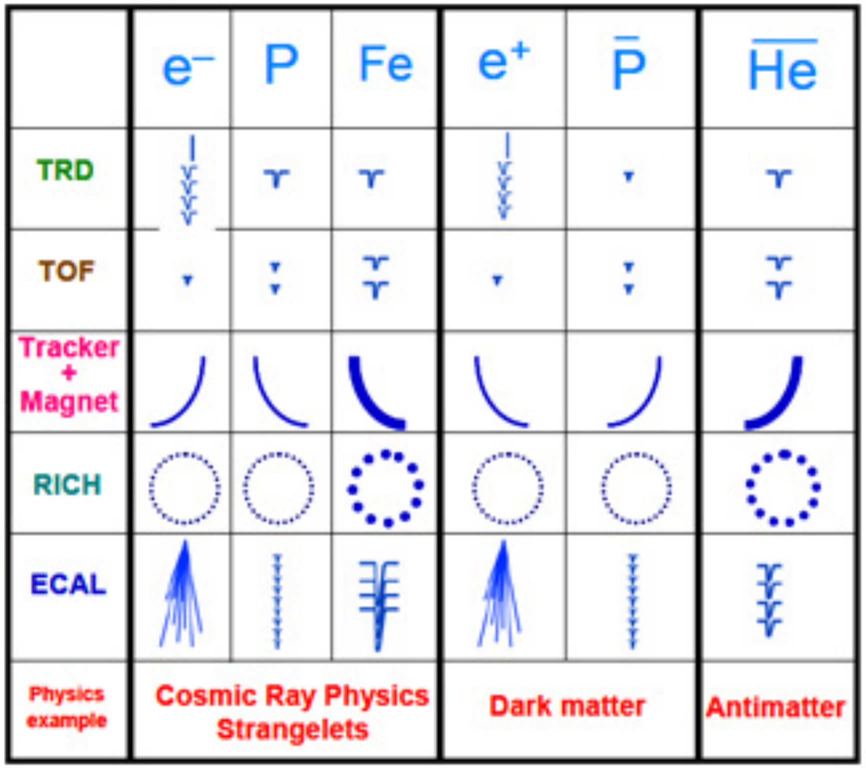

AMS – discrimination - I

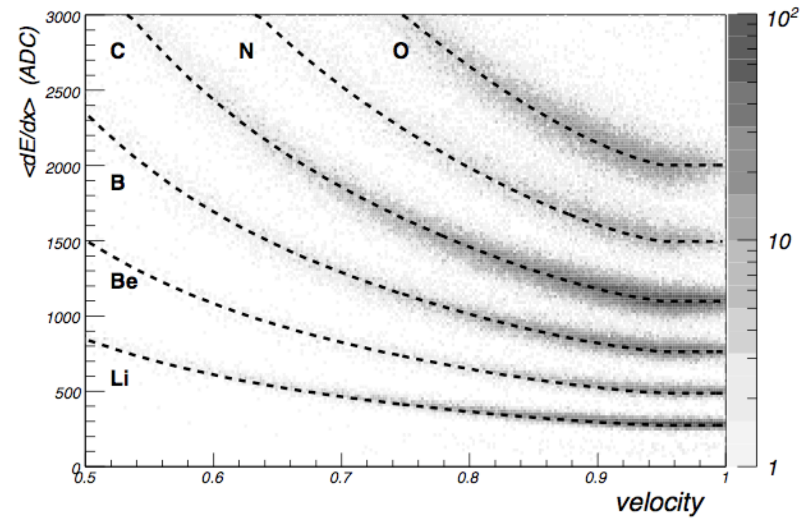

Fig. 2: Signal amplitude (ADC) of the mean energy loss in the silicon tracker vs velocity. Nuclear families fall into distinct charge bands. MPVs of the $P_Z^k(x_k, \beta)$ functions are superimposed for Z=3 to 8 (dashed lines).

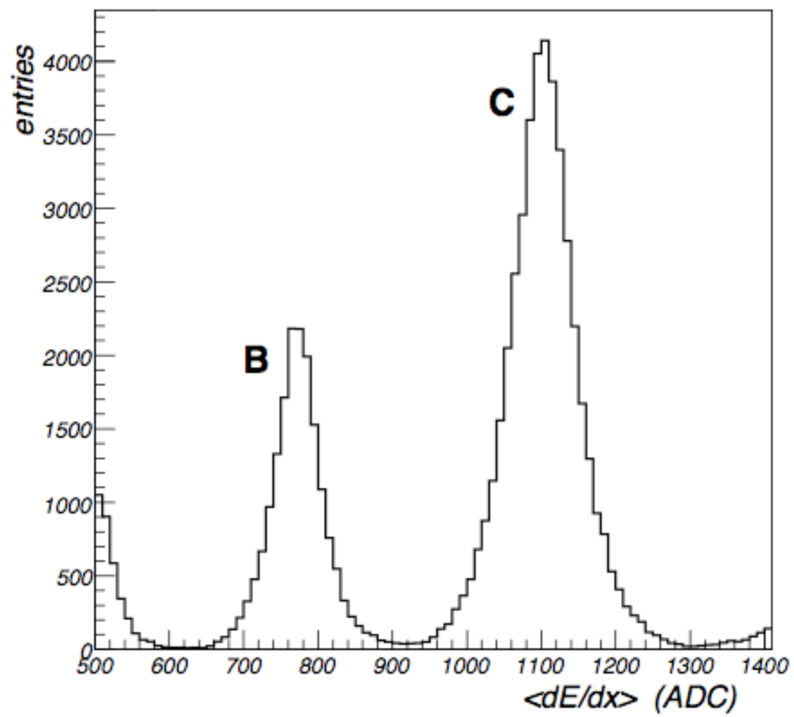

Fig. 3: Charge histograms in the B and C region. The signal amplitudes of Fig.2 are here equalized to $\beta \equiv 1$. Boron and Carbon families fall in distinct charge peaks.

AMS – discrimination - II

TRD estimator:
LogL(electron)/LogL(proton)

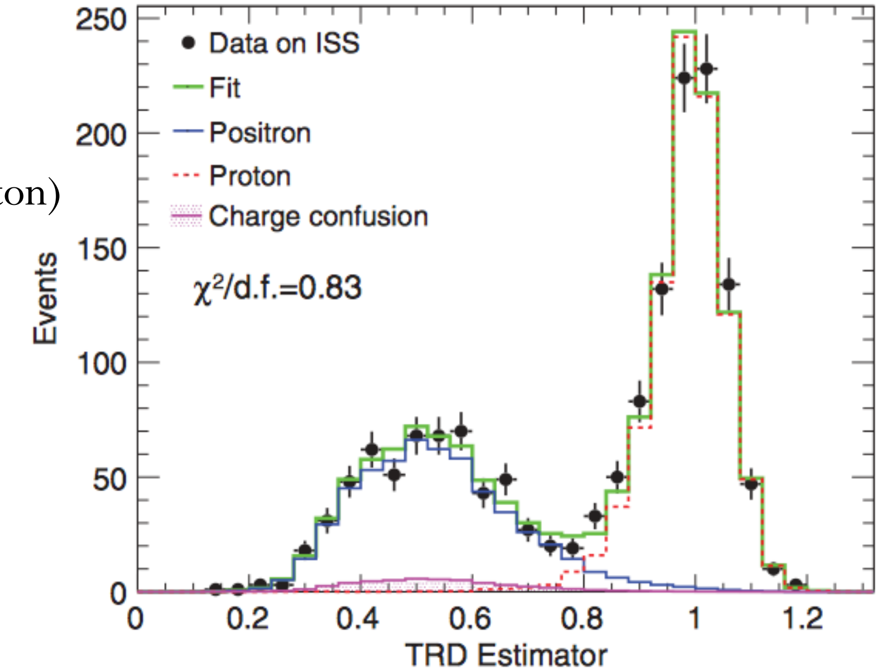

FIG. 3 (color). Separation power of the TRD estimator in the energy range 83.2–100 GeV for the positively charged selected data sample. For each energy bin, the positron and proton reference spectra are fitted to the data to obtain the numbers of positrons and protons.

AMS – most important result

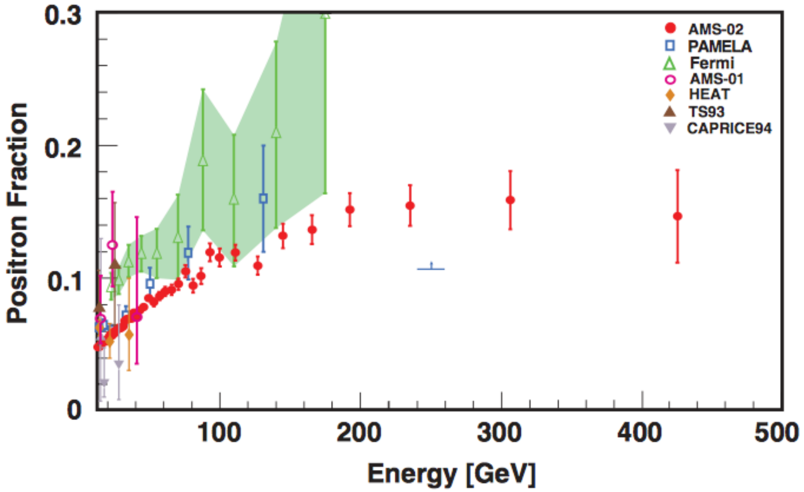

FIG. 3 (color). The positron fraction above 10 GeV, where i begins to increase. The present measurement extends the energ range to 500 GeV and demonstrates that, above ~200 GeV, th positron fraction is no longer increasing. Measurements fror PAMELA [21] (the horizontal blue line is their lower limit) Fermi-LAT [22], and other experiments [17–20] are also showr

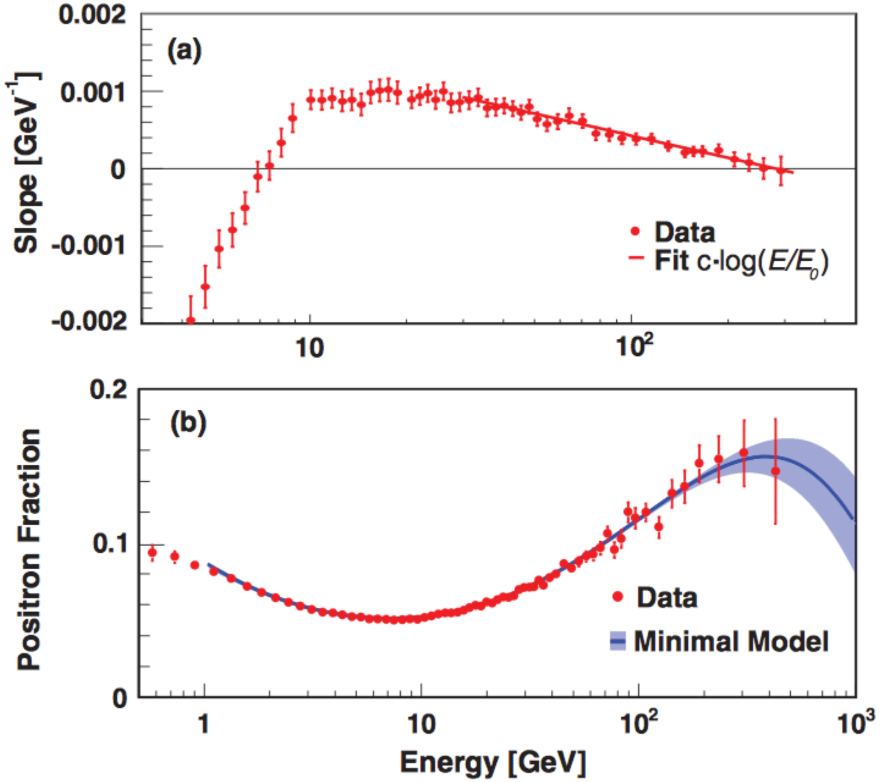

FIG. 4 (color). (a) The slope of the positron fraction vs energy over the entire energy range (the values of the slope below 4 GeV are off scale). The line is a logarithmic fit to the data above 30 GeV. (b) The positron fraction measured by AMS and the fit of a minimal model (solid curve, see text) and the 68% C.L. range of the fit parameters (shaded). For this fit, both the data and the model are integrated over the bin width. The error bars are the quadratic sum of the statistical and systematic uncertainties. Horizontally, the points are placed at the center of each bin.

MEG - I

- Detect the Lepton Violating Decay $\mu \rightarrow e\,\gamma$
- Motivation:
  - Never observed (BR<1.2×10^{-11})
  - Supersymmetry predicts a possible signal "just around the corner": aim to reach O(10^{-13})
- How to build an experiment ?
  - source of muons, no need of high energy, better having muons at rest ➔ stop muons in a target
  - tw-body decay: monochromatic back-to-back electrons and gammas

$$p_e = p_\gamma = \frac{m_\mu^2 - m_e^2}{2m_\mu} \approx \frac{m_\mu}{2} \approx 52 MeV$$

MEG - II

- $\approx$ 20 MeV/c positive muons from a proton-pion beam:
  - 10^8 μ/s rate (PSI beam)
  - large effort to have a clean beam, without halos, and with muons only (all other beam components are reduced to negligible levels)
- 205 μm thick polyethilene target (ρ=0.9 g/cm^3) for stopping muons (t = 0.018 g/cm^2 for orthogonal tracks)
  - very thin to reduce γ conversion and e^+ annihilations and multiple scattering;
  - thick enough in such a way that most muons stop. Range of 20 MeV/c muons is $\approx$ 0.05 g/cm^2 . An option is to have a inclined target.
- The apparatus requires:
  - a detector to identify 52 MeV photons
  - a detector to identify 52 MeV/c positrons
  - strong rejection powers vs. background (see later)

MEG - III

- Backgrounds
  - $\mu \rightarrow e\nu\nu$
  - $\mu \rightarrow e\nu\nu\gamma$
  - accidentals $\mu \rightarrow e\nu\nu$ + independent γ production (positron annihilation or radiative decay,…)
- 5 discriminating variables for the analysis:
  - Energies: $\boldsymbol{E_e}$, $\boldsymbol{E_\gamma}$ (the signal requires them to be fixed at ≈ 52 MeV)
  - Angles between e and γ: $\boldsymbol{\theta_{e\gamma}}$, $\boldsymbol{\phi_{e\gamma}}$ (the signal requires them to be close to 0, back-to-back)
  - Emission time difference between e and γ: $\boldsymbol{t_{e\gamma}}$(the signal requires it to be 0, they are produced simultaneously).

MEG - IV

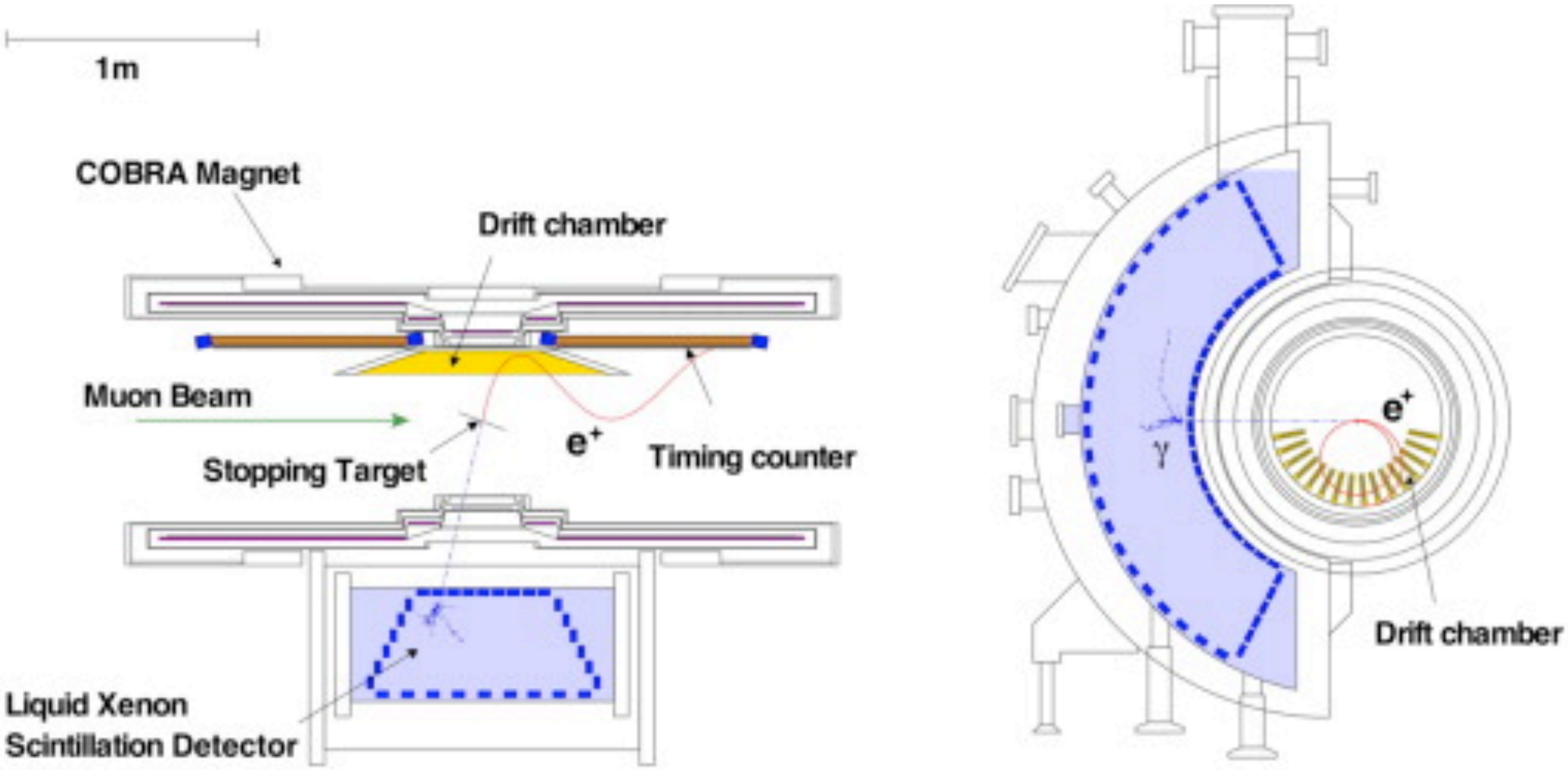

1m
COBRA Magnet
Drift chamber
Muon Beam
Stopping Target
e+
Timing counter
Liquid Xenon
Scintillation Detector
γ
e+
Drift chamber

MEG - V

- Detectors:
  - Liquid Xenon Calorimeter for γ detection and energy and time measurement.
    - $\sigma(E_\gamma) = 1.5\%$ @ 52 MeV
    - $\sigma(t_\gamma) = 69$ ps
  - Tracking chamber in a non-uniform magnetic field to measure positron trajectory and momentum.
    - $\sigma(r) = 200\ \mu m$; $\sigma(z) = 800\ \mu m$; $\sigma(\theta) = 9$ mrad
    - $\sigma(p) = 0.33\ (1.56)$ MeV @52 MeV
  - Time-of-flight counters to measure positron timing.
    - $\sigma(t_e) = 70$ ps

$\sigma_E \sim 1.9\%$ @ 52.8 MeV

$\sigma_{xy} \sim 5 - 6$ mm

$\sigma_T \sim 60$ ps

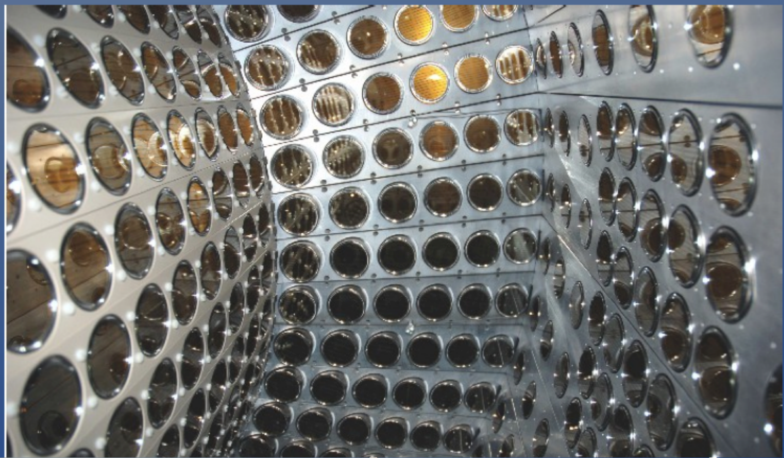

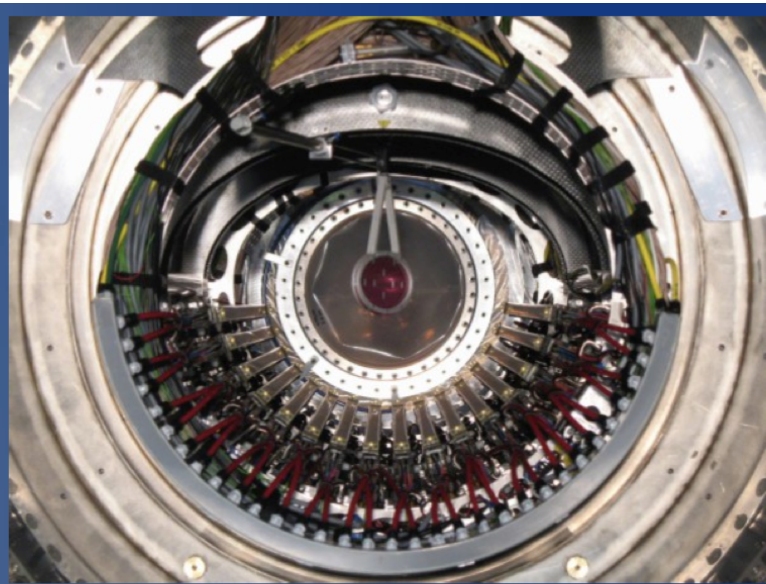

Tracking performances

$\sigma_P \sim 300$ keV

$\sigma_{vtx} \sim 1.2$ (x), 2.4 (y)

$\sigma_{\theta,\varphi} \sim 9$ mrad

2 x 15 scintillating bars for trigger and positron timing ($\sigma_T \sim 60$ ps)

2 x 256 fibers to measure the z coordinate

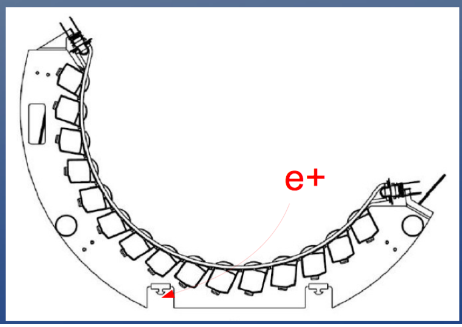

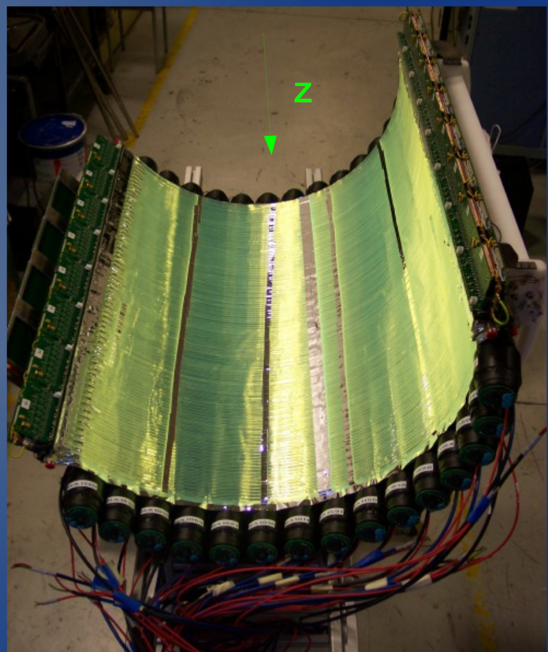

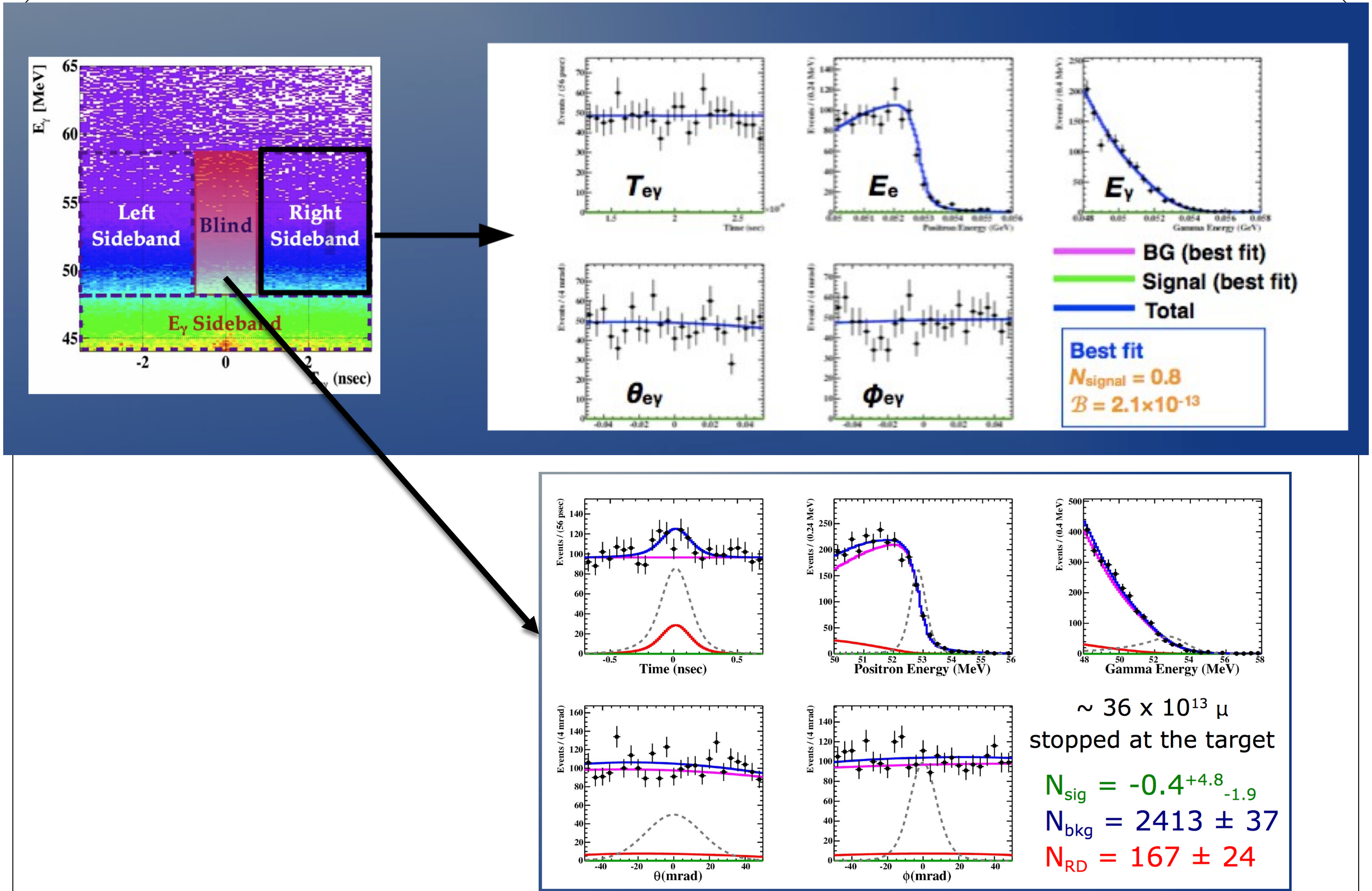

Left Sideband
Blind
Right Sideband
Eγ Sideband
Eγ [MeV]
Tγ (nsec)
Teγ
Ee
Eγ
θeγ
φeγ
BG (best fit)
Signal (best fit)
Total
Best fit
Nsignal = 0.8
B = 2.1×10-13
Time (nsec)
Positron Energy (MeV)
Gamma Energy (MeV)
θ(mrad)
φ(mrad)
~ 36 x 10^13 μ stopped at the target
Nsig = -0.4 +4.8 -1.9
Nbkg = 2413 ± 37
NRD = 167 ± 24

MEG - VI

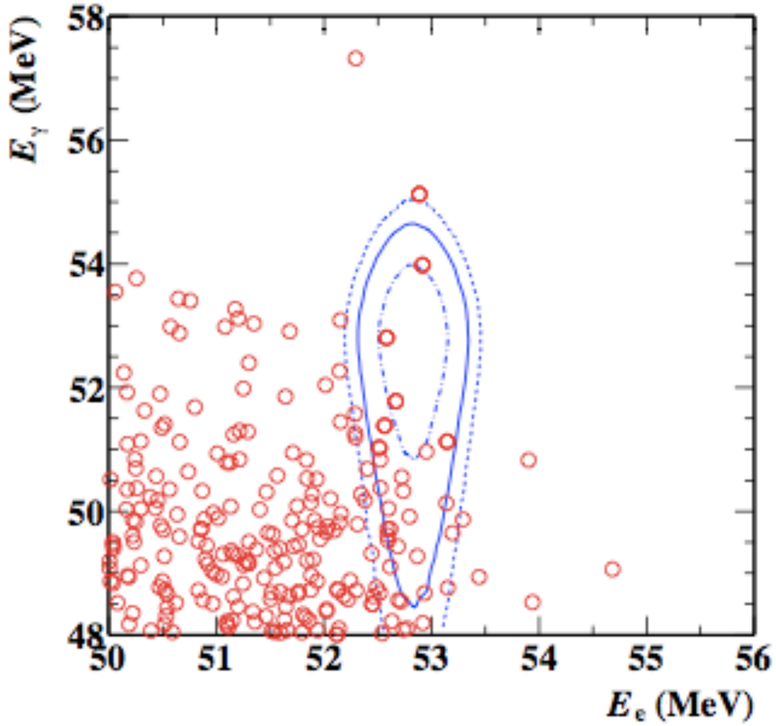

E_γ (MeV)
58
56
54
52
50
48
50
51
52
53
54
55
56
E_e (MeV)

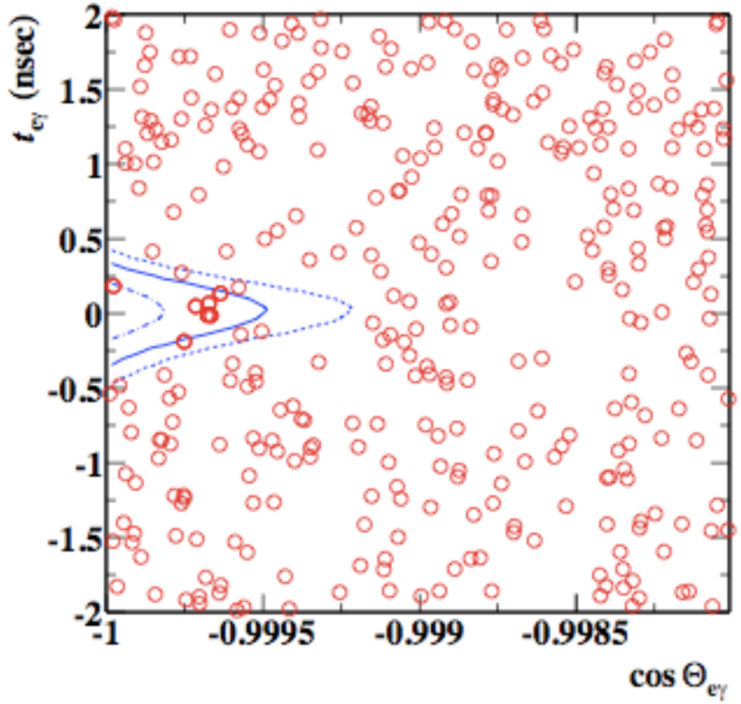

$t_{e\gamma}$ (nsec)
2
1.5
1
0.5
0
-0.5
-1
-1.5
-2
-1
-0.9995
-0.999
-0.9985
$\cos\Theta_{e\gamma}$

SNO – A "smart" solar neutrino experiment.

- Solar neutrino problem: the electron neutrino flux coming from the sun is "lower" than the flux expected from the solar model
  - the solar model is wrong;
  - the neutrinos oscillate during the travel.
- The idea of SNO is: we built a detector able to measure neutrinos from the sun, BUT not only electron neutrinos, also muon and tau neutrinos. This can be done detecting 3 different reactions:
  - $\nu + d \rightarrow p + p + e^-$ (CC – only ν_e)
  - $\nu + d \rightarrow p + n + \nu$ (NC – all three flavours)
  - $\nu + e^- \rightarrow \nu + e^-$ (ES – all three flavours BUT different rates)
- A deuterium target (Heavy water tank) helps if I can detect electrons or neutrons from the very rare reactions
- Going deeply underground helps to reduce the background

SNO – few numbers

- Neutrinos from the sun are few MeV neutrinos, cross-sections are ≈ 10^{-42} cm^2 (very small)
- Neutrinos from the sun fluxes are of the order of ≈ 10^6 cm^{-2}s^{-1}.
- How many neutrino interactions can I get, given an amount of deuterium nuclei ?

$$\dot{N} = \sigma_\nu \varphi N_d \approx 10^{-36} N_d (s^{-1})$$

- If I want at least O(10^3) events in one year O(10^7 s) we need:

$$N_d \approx 10^{32}$$

- How can I get a sample of 10^{32} deuterium nuclei ? A tank of 1000 tonns of heavy water contains

$$N_d = 2\frac{M}{M_{D2O}} \approx \frac{2\times 10^6 Kg}{20\times m_N} = 6\times 10^{31}$$

SNO - detector

- Logic: tank of 1000 tonns of heavy water and PMT to see Cerenkov light
  - from electrons in case of ES and CC reactions
  - from 6.25 MeV γ from capture of neutrons from detuterium in case of NC reactions (after thermalization of the neutron)
  - The three reactions can be disentangled in terms of three measurements:
    - Energy (of electrons and of gamma through Compton or pair production)
    - Radius (in terms of $(R/R_{AV})^3$, uniformity of the scattering position)
    - $\cos\theta_{sun}$ (depends on the correlation btw electron directions and primary neutrinos)

SNO – detector sketch

Main features:

2070m below ground in INCO's Creighton mineDeep Sudbury mine

Heavy water tank 1000 tonns

Light water envelope 7000 tonns

Sphere of 10000 PMTs around the envelope (inward and backward)

High water purity with controlled quantity of NaCl in Heavy Water tank (to enhance NC detection)

Each PMT measures charge and Time

➔ Cerenkov ring ➔ direction and energy

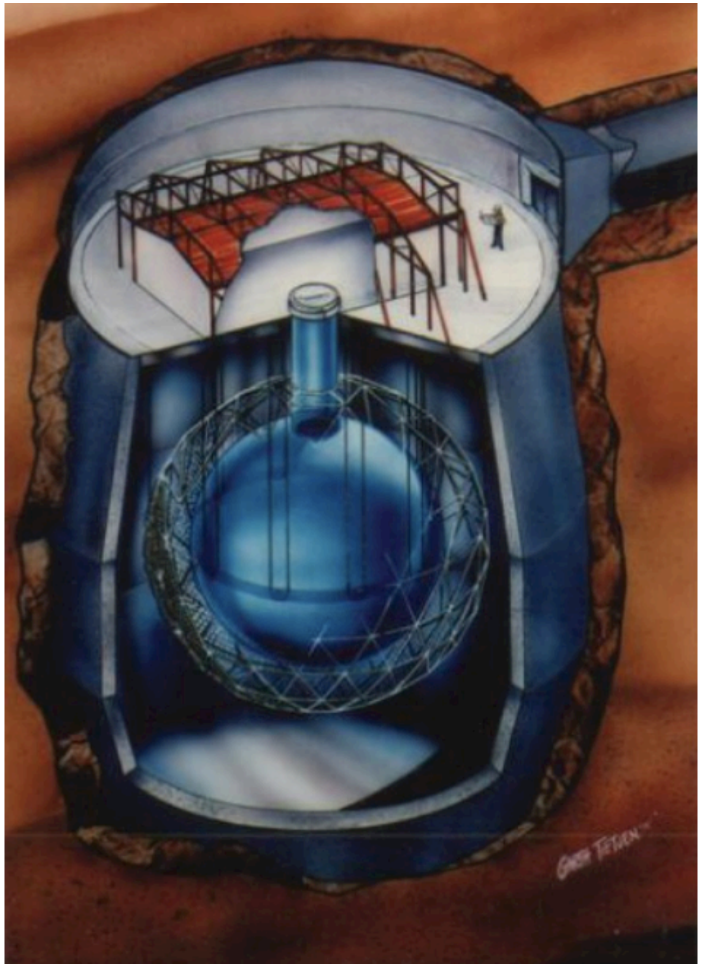

SNO event

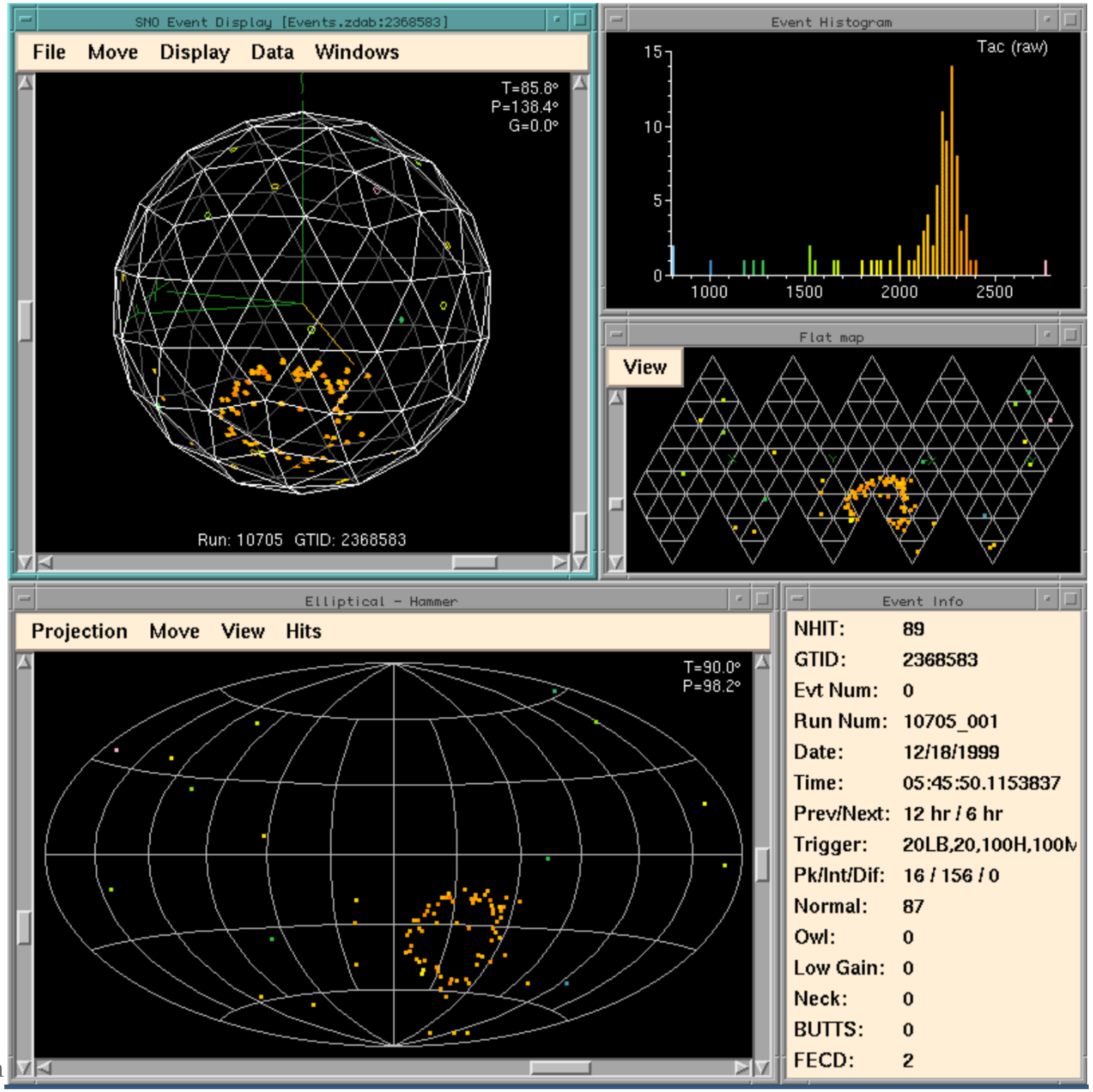

SNO Event Display [Events.zdab:2368583]
File Move Display Data Windows
T=85.8°
P=138.4°
G=0.0°
Run: 10705 GTID: 2368583
Event Histogram
Tac (raw)
15
10
5
0
1000
1500
2000
2500
Flat map
View
Elliptical - Hammer
Projection Move View Hits
T=90.0°
P=98.2°
Event Info
NHIT: 89
GTID: 2368583
Evt Num: 0
Run Num: 10705_001
Date: 12/18/1999
Time: 05:45:50.1153837
Prev/Next: 12 hr / 6 hr
Trigger: 20LB,20,100H,100M
Pk/Int/Dif: 16 / 156 / 0
Normal: 87
Owl: 0
Low Gain: 0
Neck: 0
BUTTS: 0
FECD: 2

SNO – variables used

Energy

NB solar neutrinos energies

E_ν<15 MeV

Radius

Direction

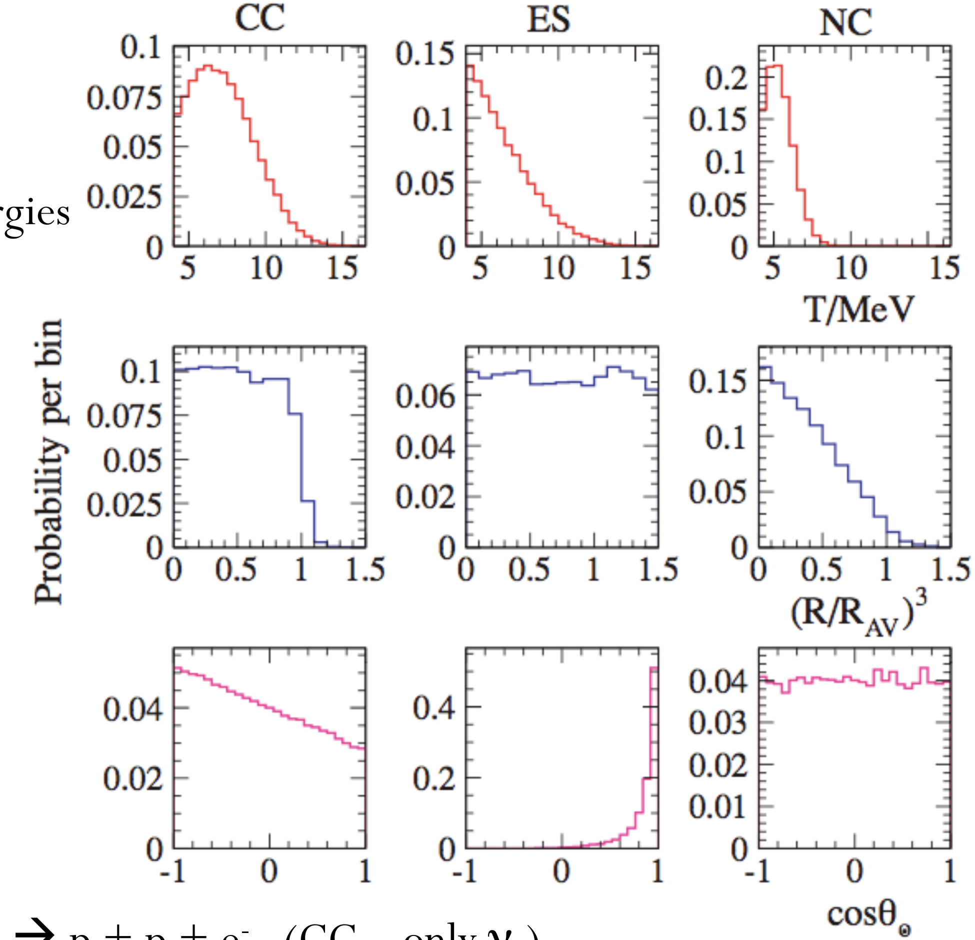

$\nu + d \rightarrow p + p + e^-$ (CC – only ν_e)

$\nu + e^- \rightarrow \nu + e^-$ (ES – all three flavours BUT different rates)

$\nu + d \rightarrow p + n + \nu$ (NC – all three flavours)

SNO - results

$$\phi_{CC} = \phi(\nu_e),$$
$$\phi_{ES} = \phi(\nu_e) + 0.1559\phi(\nu_{\mu\tau}),$$
$$\phi_{NC} = \phi(\nu_e) + \phi(\nu_{\mu\tau}),$$

$$\phi_{CC} = 1.76^{+0.06}_{-0.05}\,(\text{stat.})^{+0.09}_{-0.09}\,(\text{syst.}) \times 10^6\ \text{cm}^{-2}\text{s}^{-1},$$
$$\phi_{ES} = 2.39^{+0.24}_{-0.23}\,(\text{stat.})^{+0.12}_{-0.12}\,(\text{syst.}) \times 10^6\ \text{cm}^{-2}\text{s}^{-1},$$
$$\phi_{NC} = 5.09^{+0.44}_{-0.43}\,(\text{stat.})^{+0.46}_{-0.43}\,(\text{syst.}) \times 10^6\ \text{cm}^{-2}\text{s}^{-1},$$
$$\phi(\nu_e) = 1.76^{+0.05}_{-0.05}\,(\text{stat.})^{+0.09}_{-0.09}\,(\text{syst.}) \times 10^6\ \text{cm}^{-2}\text{s}^{-1},$$
$$\phi(\nu_{\mu\tau}) = 3.41^{+0.45}_{-0.45}\,(\text{stat.})^{+0.48}_{-0.45}\,(\text{syst.}) \times 10^6\ \text{cm}^{-2}\text{s}^{-1}.$$

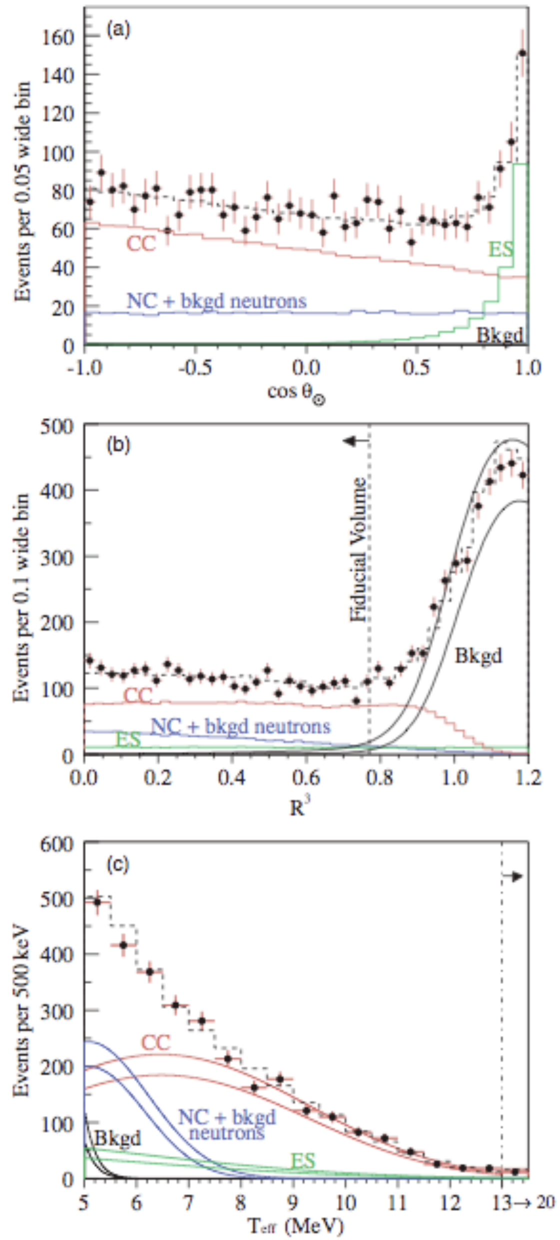

SNO – result interpretation

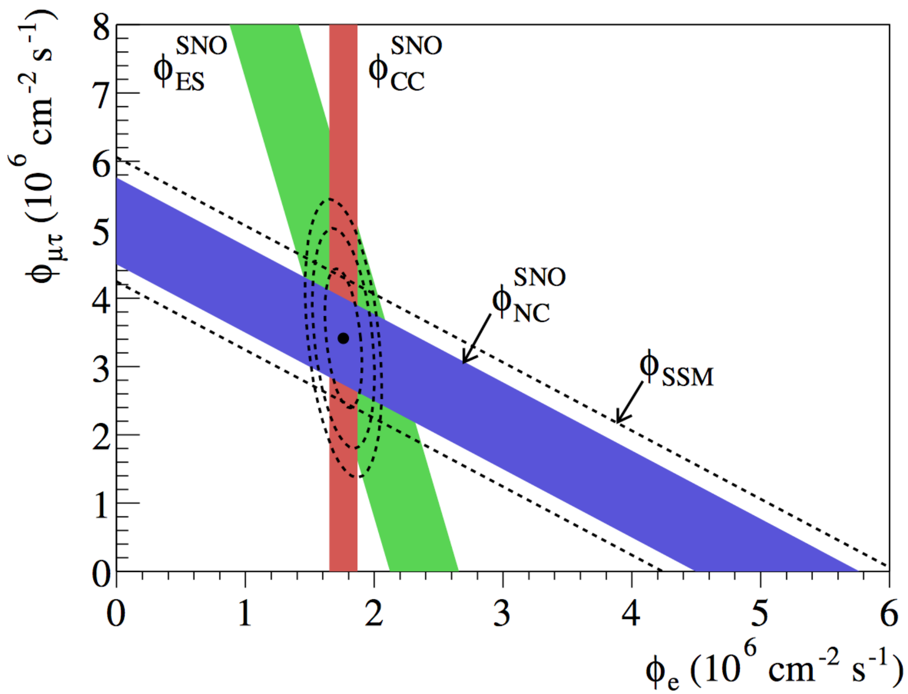

Figure 5: SNO's CC, NC and ES measurements from the D_2O phase. The x- and y-axes are the inferred fluxes of electron neutrinos and muon plus tau neutrinos. Since the NC and ES measurements are sensitive to both ν_e and ν_μ/ν_τ, the ES and NC bands have definite slopes. The CC measurement is sensitive to ν_e only, so has an infinite slope. The widths of the bands represent the uncertainties of the measurements. The intersection of the three bands gives the best estimate of $\phi_{\mu\tau}$ and ϕ_e. The dashed ellipses around the best fit point give the 68%, 95%, and 99% confidence level contours for $\phi_{\mu\tau}$ and ϕ_e. The flux of neutrinos predicted by the SSM is indicated by ϕ_{SSM}.